

Dihydropyrimidinones: Efficient one-pot green synthesis using Montmorillonite-KSF and evaluation of their cytotoxic activity

Saleem Farooq,^{a,b*} Fahad A. Alharthi,^c Ali Alsalmeh,^c Aashiq Hussain,^d Bashir A. Dar,^e Abid Hamid,^{d,f*} S. Koul^b

^a *Department of Higher Education, Department of Chemistry, Government Degree College for Boys, Baramulla, 193101, J&K, India.*

^b *Bioorganic Chemistry Division, CSIR-Indian Institute of Integrative Medicine, Canal Road Jammu, 180001, J&K, India.*

^c *Department of Chemistry, College of Science, King Saud University, P.O. Box 2455, Riyadh, 11451, Saudi Arabia.*

^d *Cancer Pharmacology Division, CSIR-Indian Institute of Integrative Medicine, Canal Road Jammu, 180001, J&K, India.*

^e *Department of Higher Education, Department of Chemistry, Govt. Degree College Sopore, Baramulla, 193201, J&K, India.*

^f *Department of Biotechnology, Central University of Kashmir, Ganderbal, 191201, J&K, India.*

Corresponding author(s). Tel/fax: 01952-234214 (S.F.). E-mail addresses: farooqprince100@yahoo.in (Saleem Farooq).

Catalyst characterization

The crystallinity of the sample (HCNH_4) was studied by recording X-ray powder diffraction patterns on a Rigaku Miniflex diffractometer, using Ni-filtered Cu K α (0.15418 nm) radiation source (Figure 7). The sample was scanned over the range 2.00-79.99 on 2θ scale with steps 0.011° and step time 13.6 s. From the XRD prototype, it has been confirmed that the synthesized catalysts are well crystalline in nature. The powder XRD patterns of the HCNH_4 were more crystalline and show additional reflections which are characteristics of HPA. This confirmed that HPA is well supported on Montmorillonite and also improves the crystallinity of the supported catalysts. The XRD pattern of montmorillonite shows a very low intensity reflection at $2\theta=9.9$, which may be due to the residual 2:1(T-O-T) structure. The increase in specific surface area and formation of mesopores results because of delamination during the process of preparation. HPA loading on montmorillonite increases the phase crystallinity, which increases the available active acidic sites for the reactions. It is obvious that the peaks are very sharp which provide evidence that the sample is exceedingly crystalline. The B.E.T. surface area of the catalyst was determined using the instrument SMART SORB 92/93 under the liquid Nitrogen. The surface area of the catalyst is 80.4762 m^2/g . To study the morphology SEM of sample (Figure 8) was carried out using JEOL.JEM100CXII ELECTRON MICROSCOPE with ASID Accelerating Voltage 40KV. The SEM image is a confirmation for coarse surface (thus elevated surface area), which is able to absorb substrate and/ or reagent to a high extent. The SEM image of the gross morphology of the HPA/KSF is displayed in (Figure 8). It was observed that HPA particles were randomly distributed over the support surface. It should be noted that HPA layer formed in the present work was constituted by several aggregates of HPA particles and not by a continuous film.

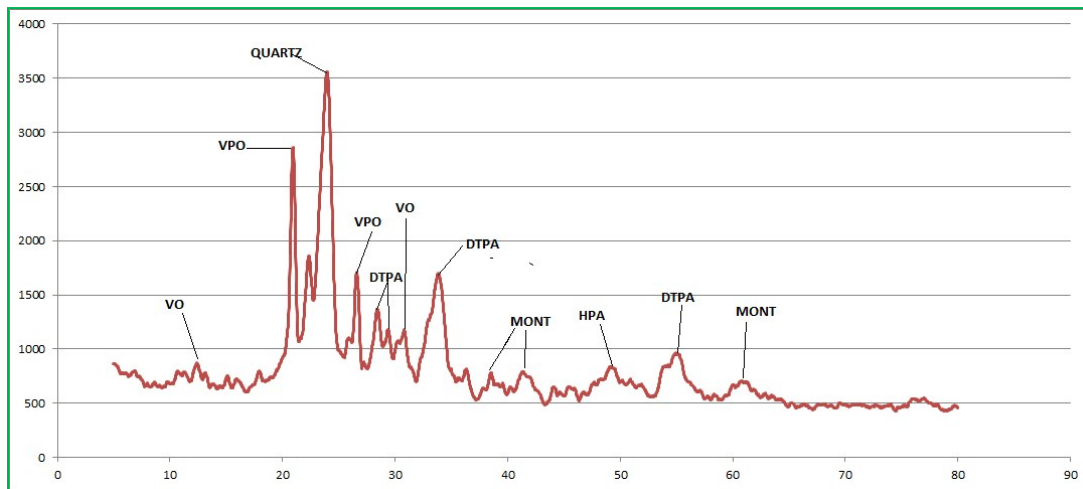


Figure S1: Powder X-ray diffraction for heteropolyacid supported on montmorillonite

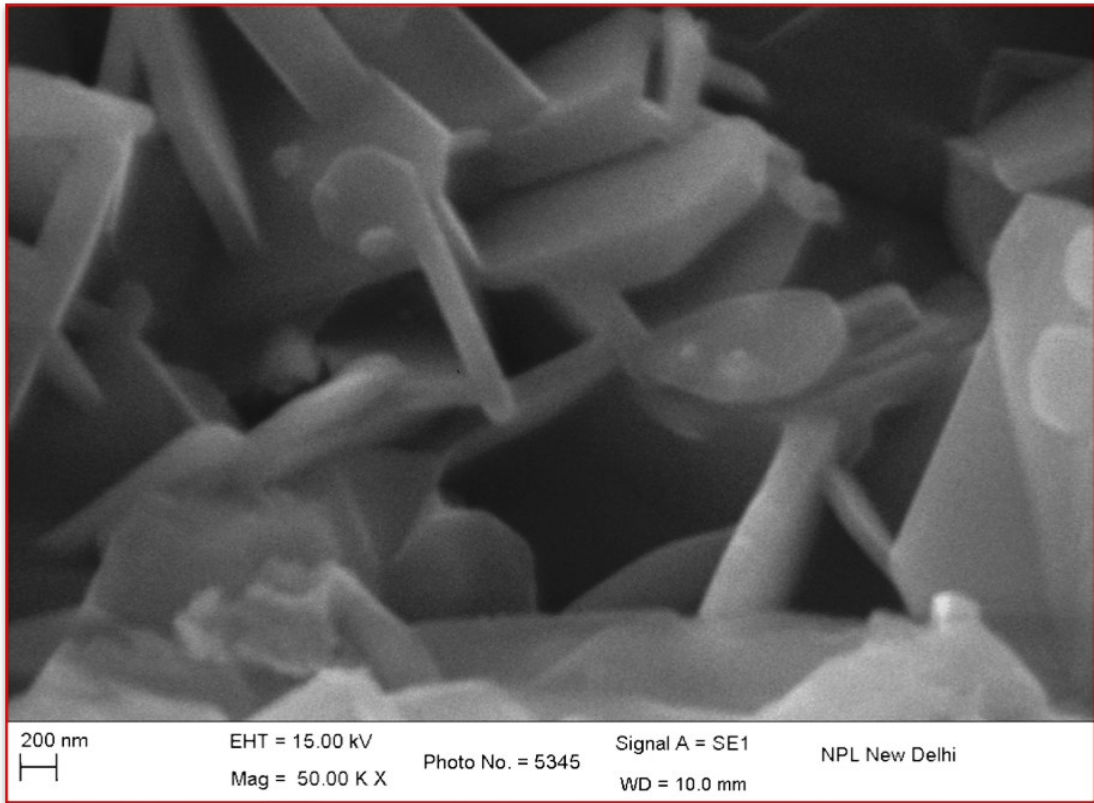


Figure S2: SEM image of Heteropolyacids clay nanocomposite

Figure S3a: Interaction figure of compound **6a** with CDK2

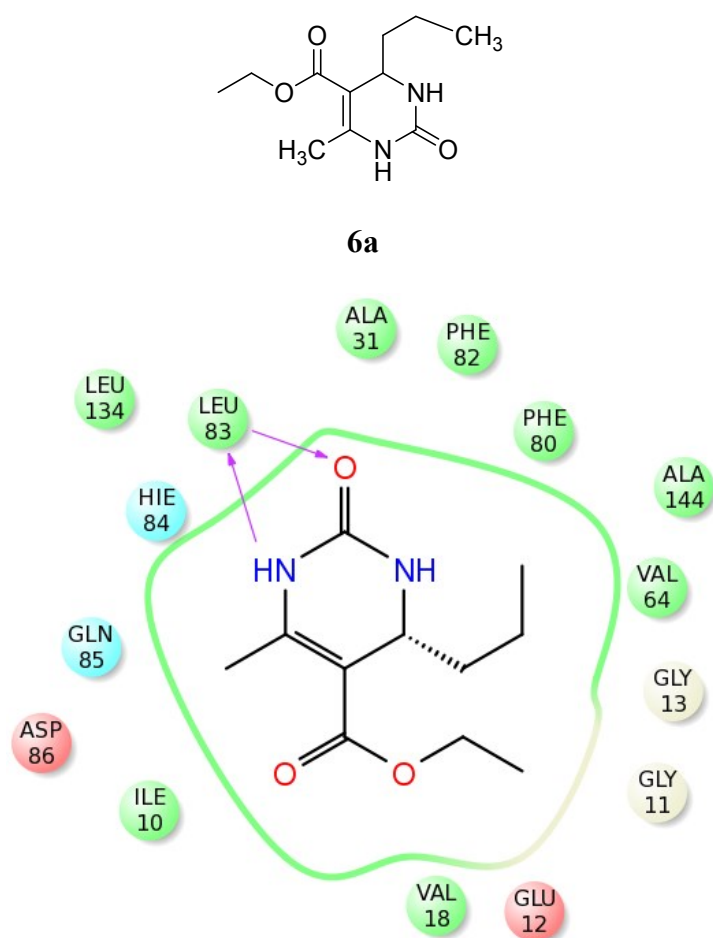


Figure S3b: Interaction figure of compound **6a** with PI3K- γ .

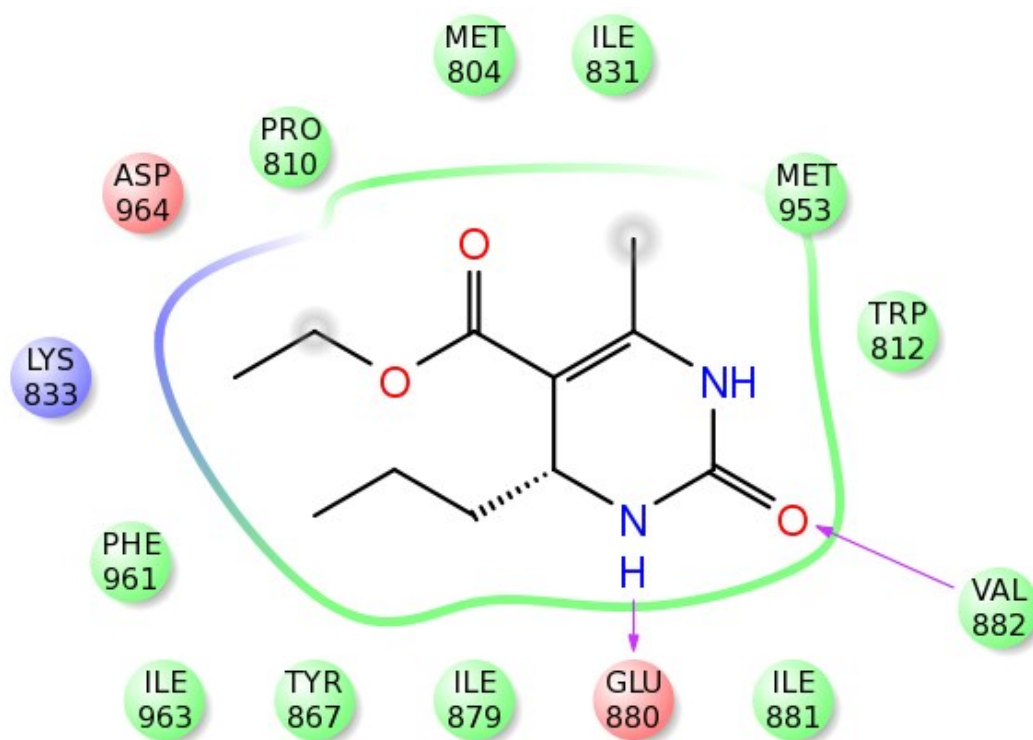


Figure S4a: Interaction figure of compound **16a** with CDK2

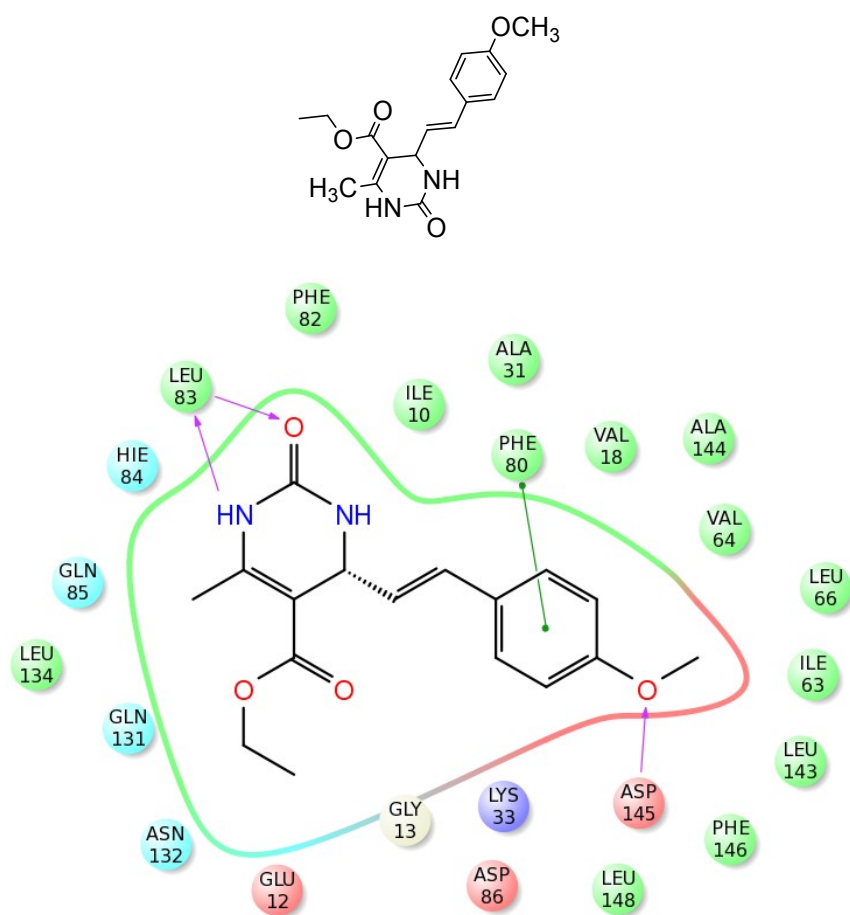


Figure S4b: Interaction figure of compound **16a** with PI3K- γ .

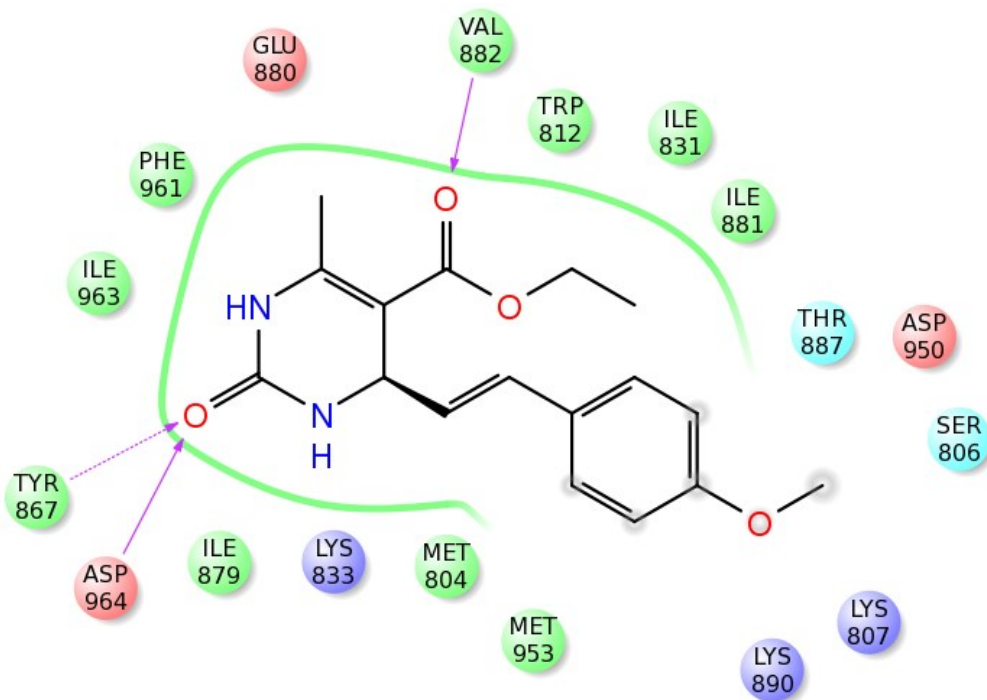
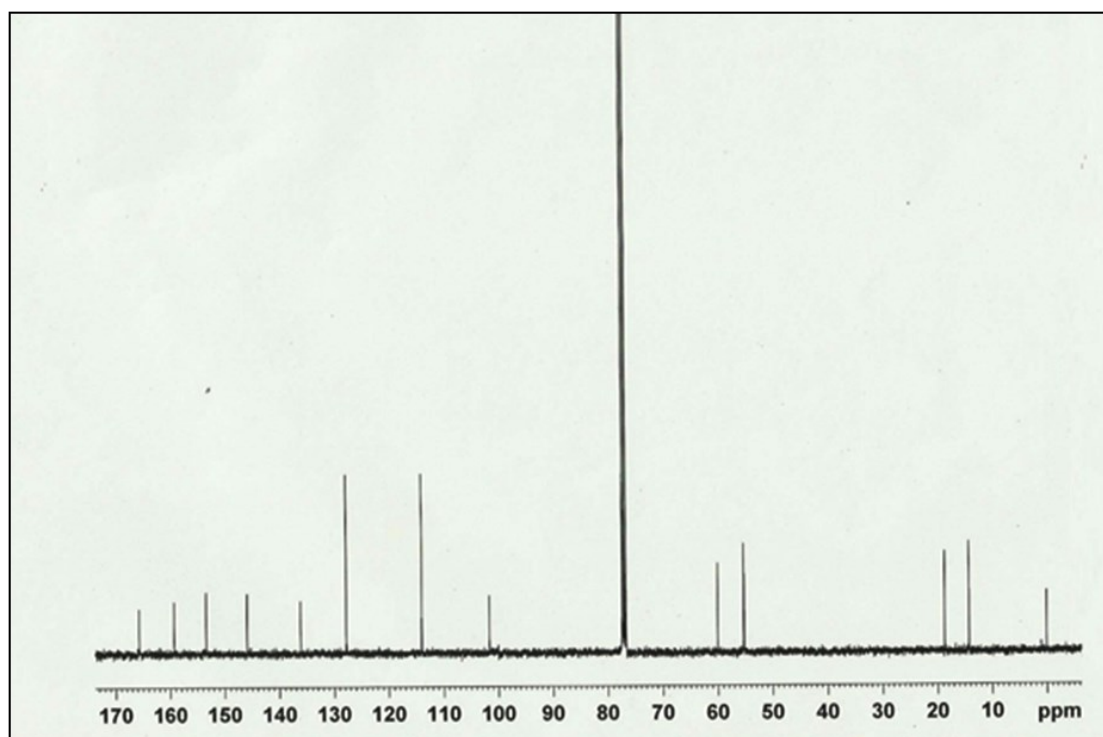
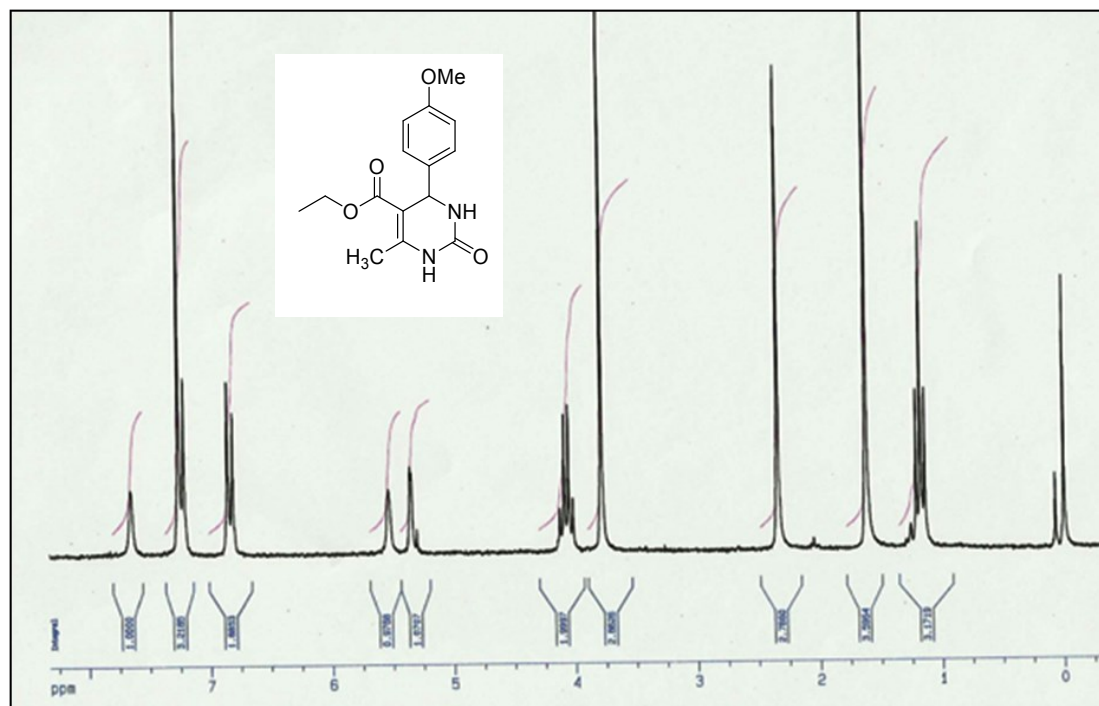
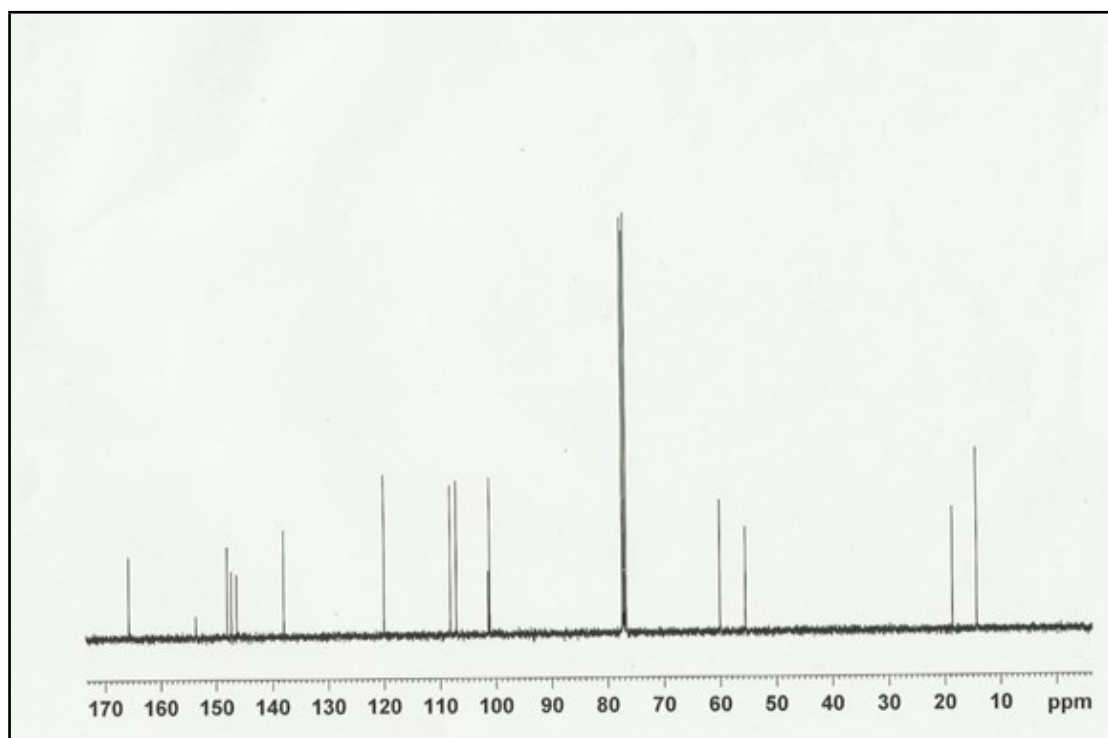
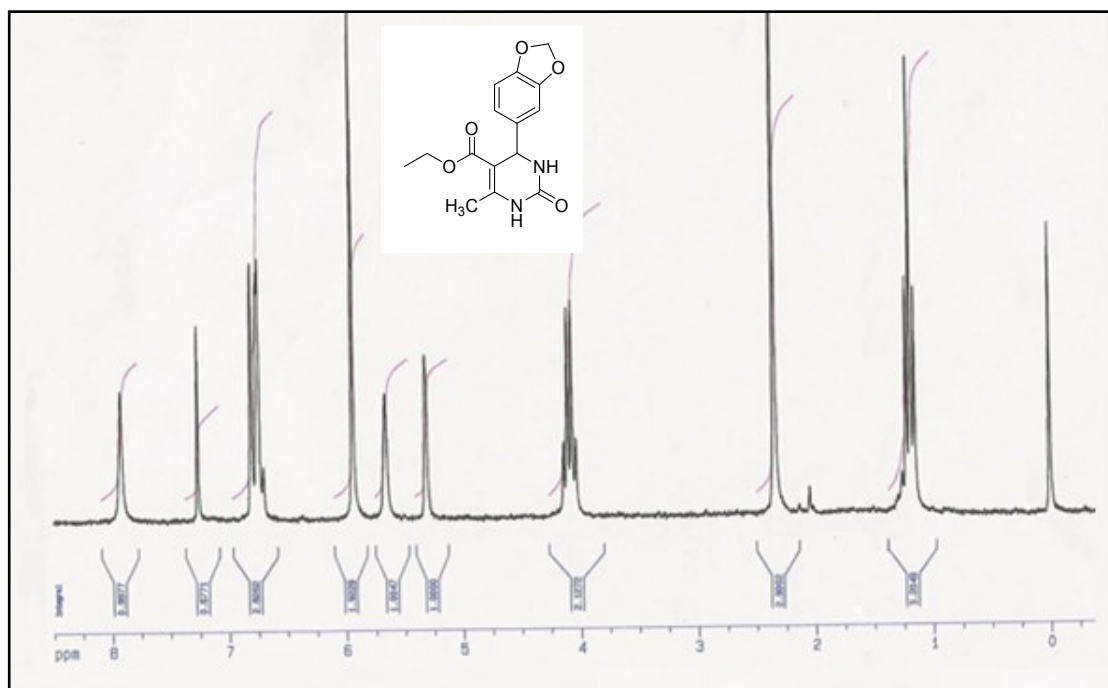


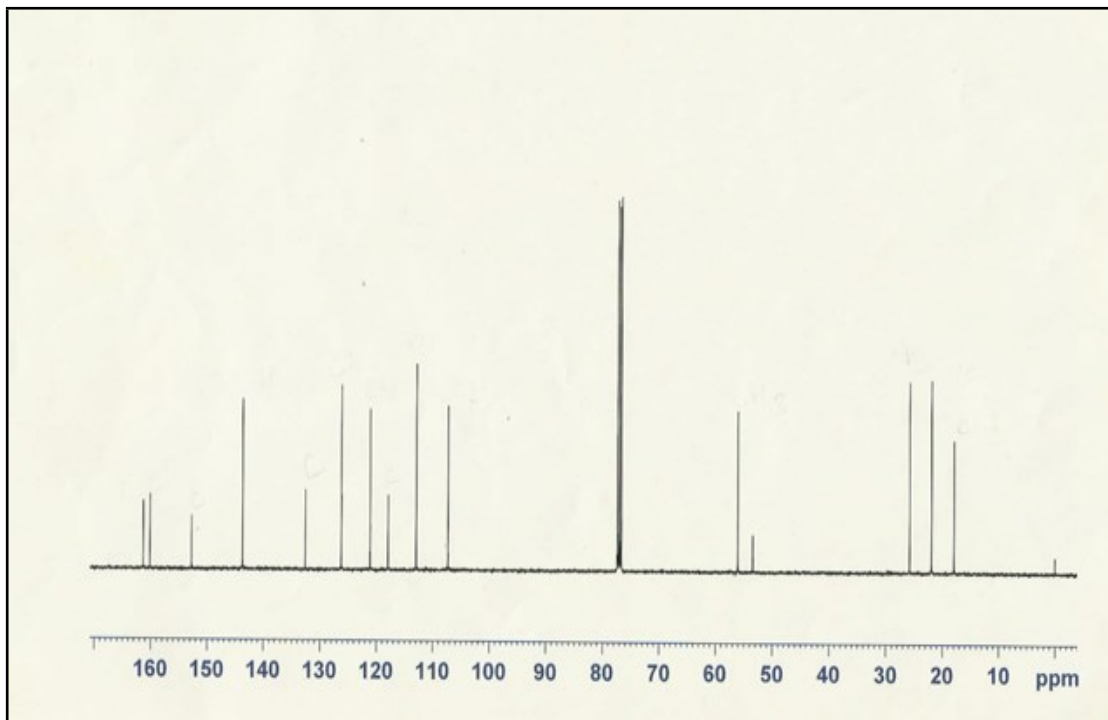
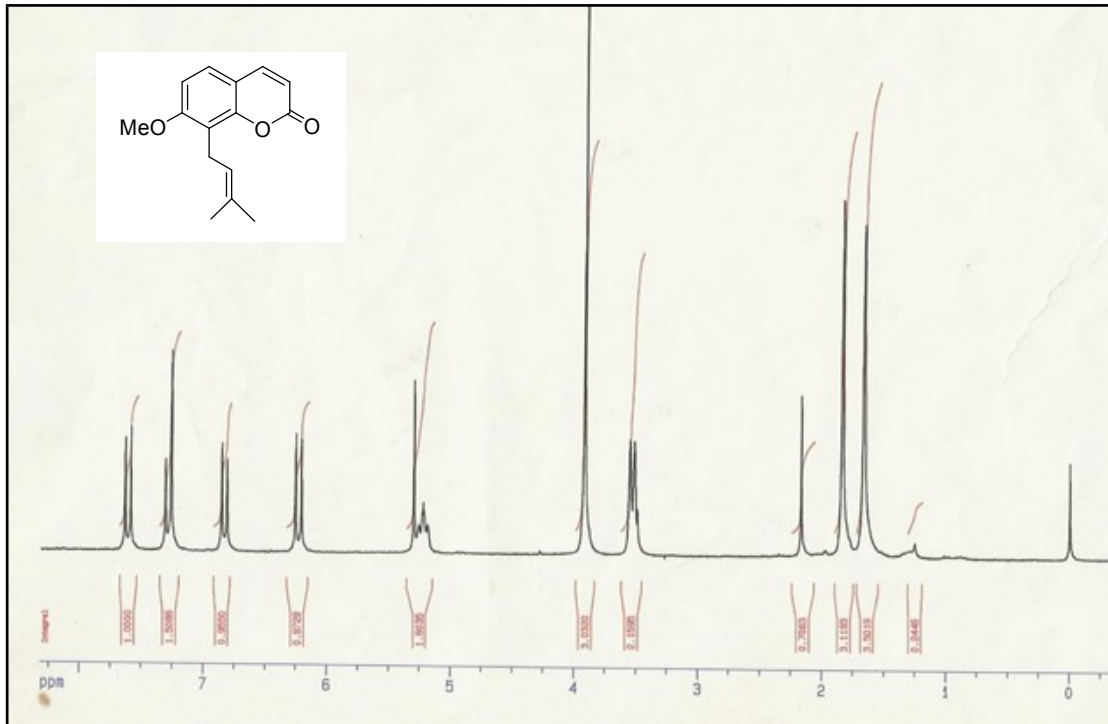
Figure S5: Spectra of Representative Compounds



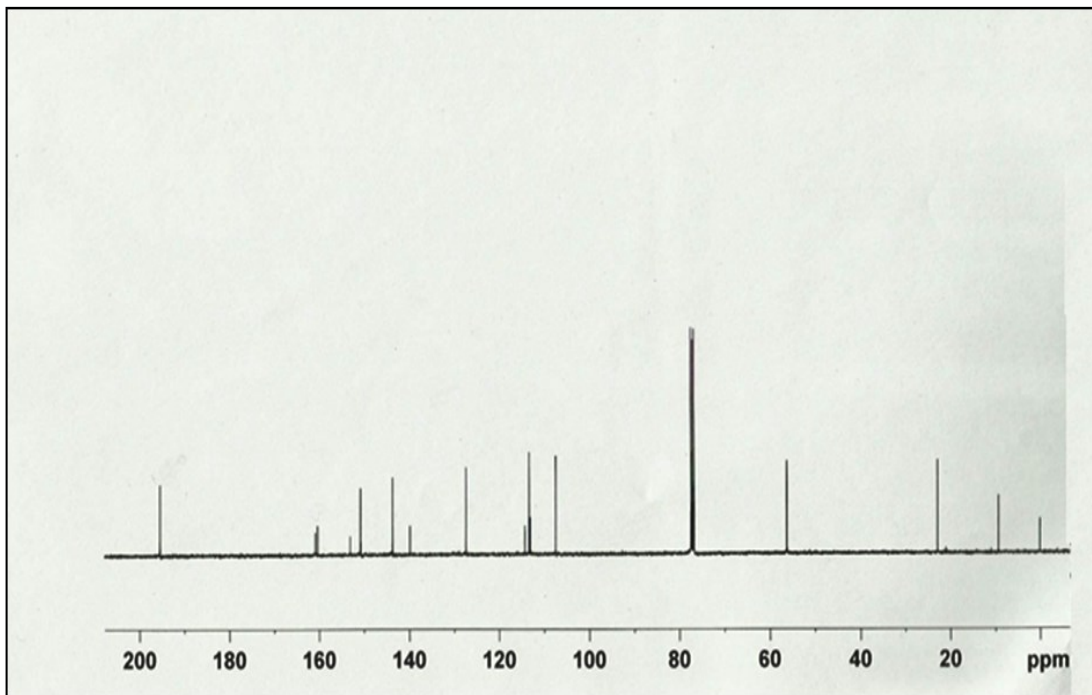
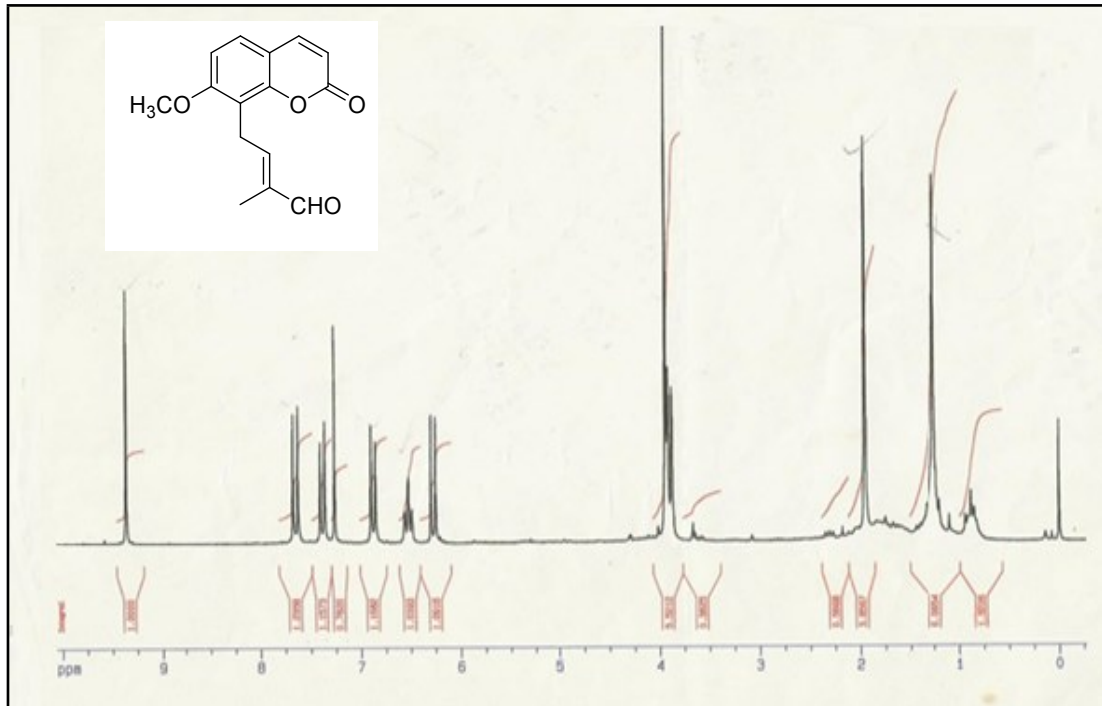
^1H & ^{13}C NMR spectra of compound (4f)



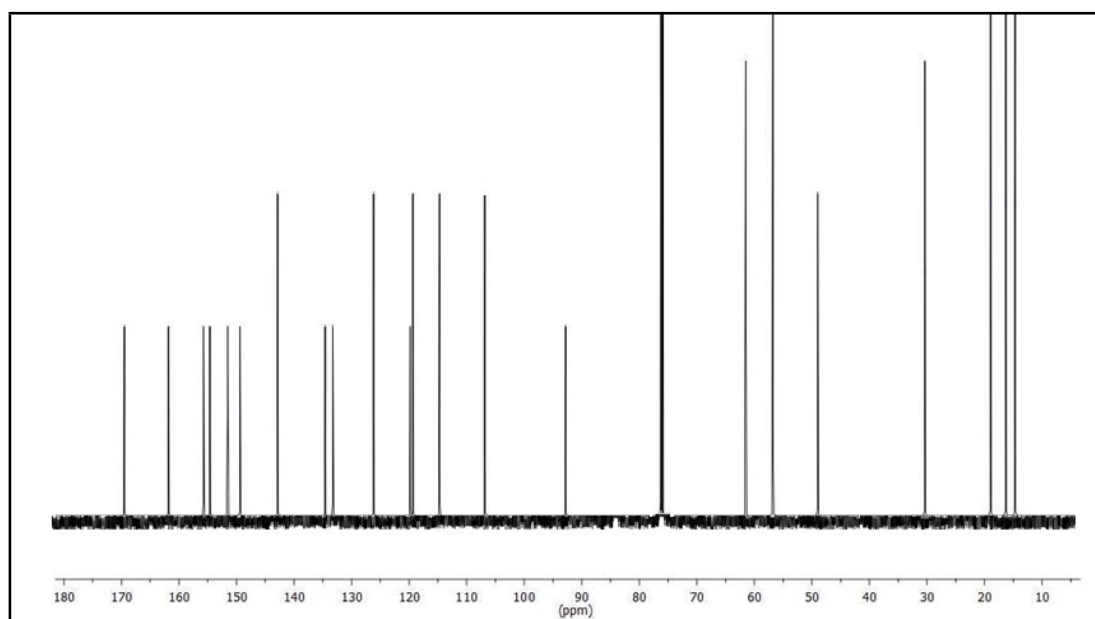
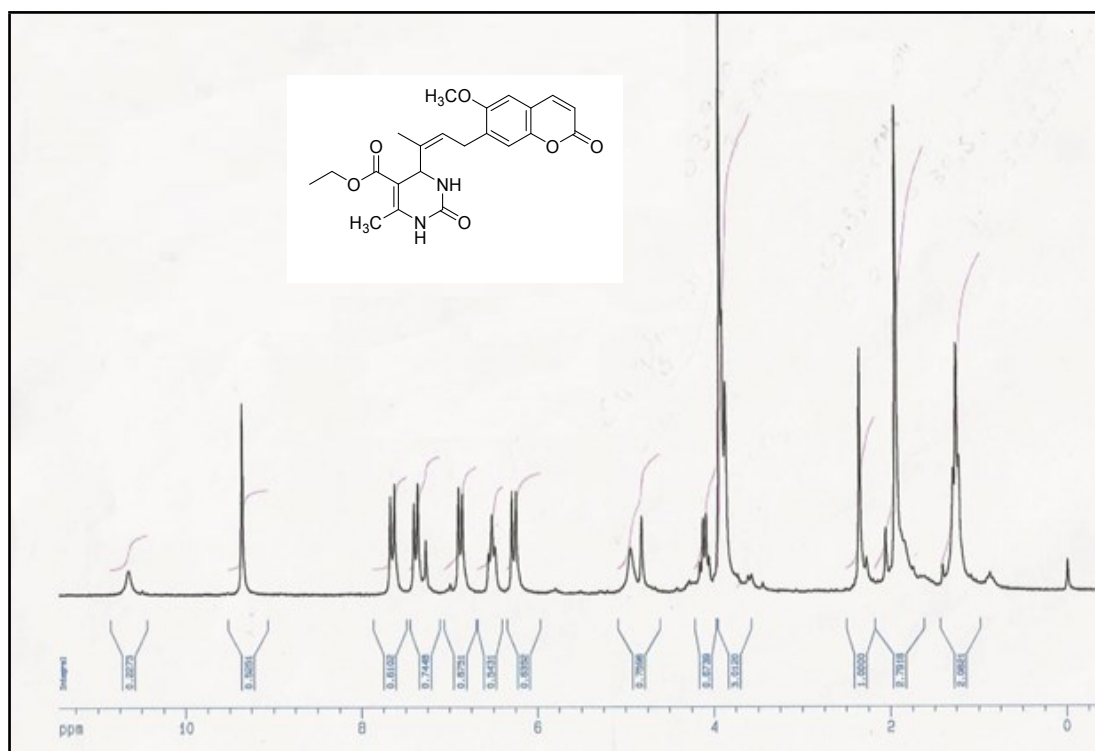
^1H & ^{13}C NMR spectra of compound (4m)



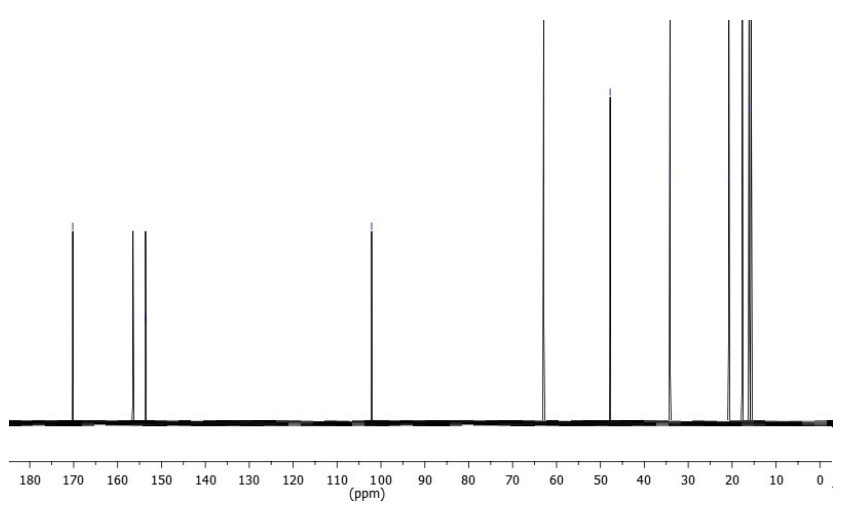
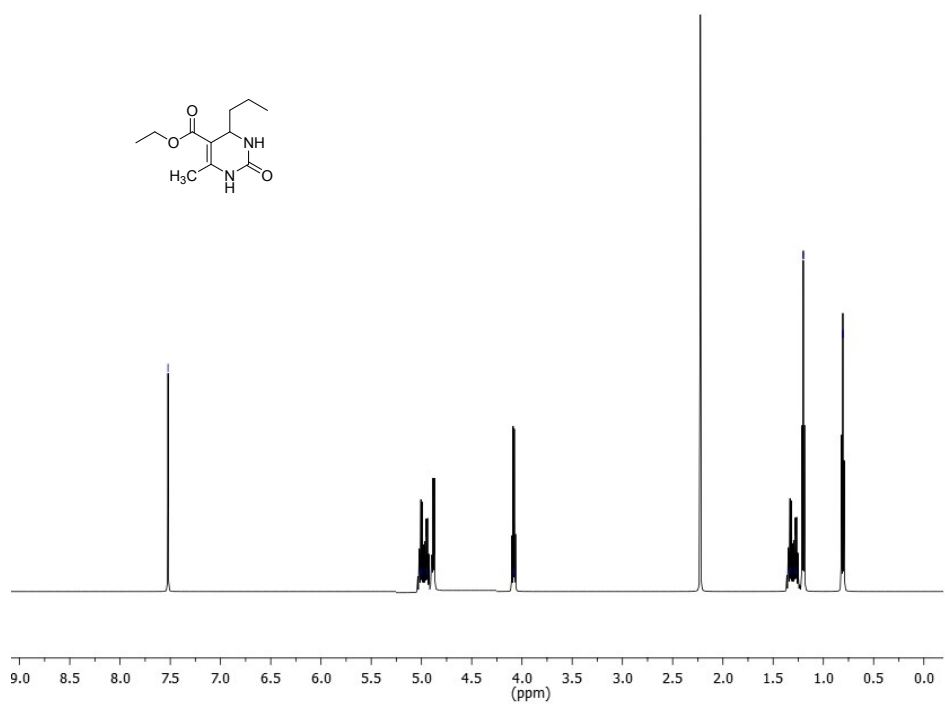
¹H & ¹³C NMR spectra of compound (osthol)



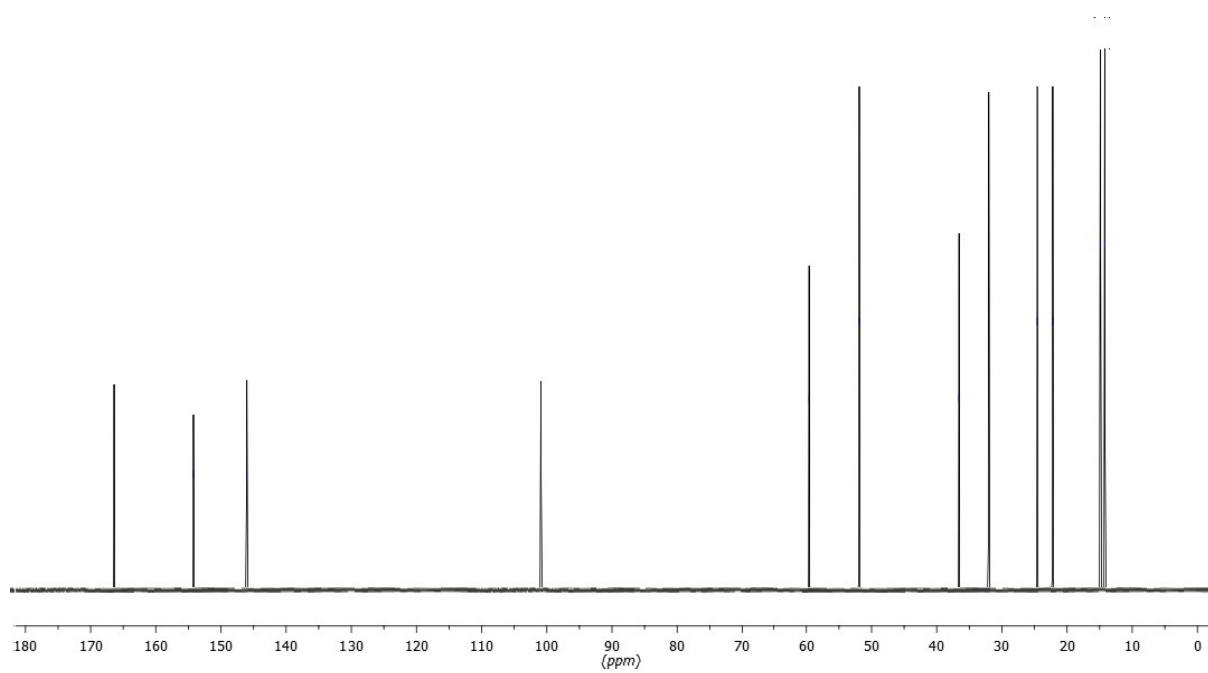
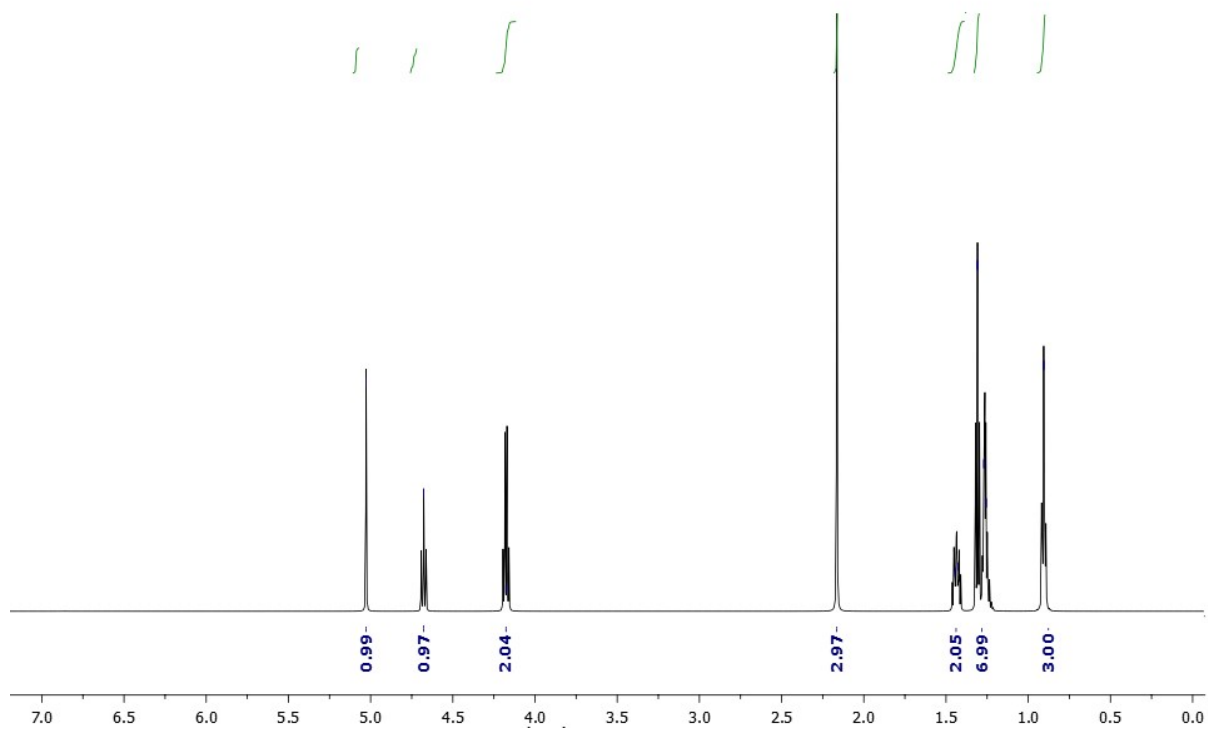
^1H & ^{13}C NMR spectra of compound (5)



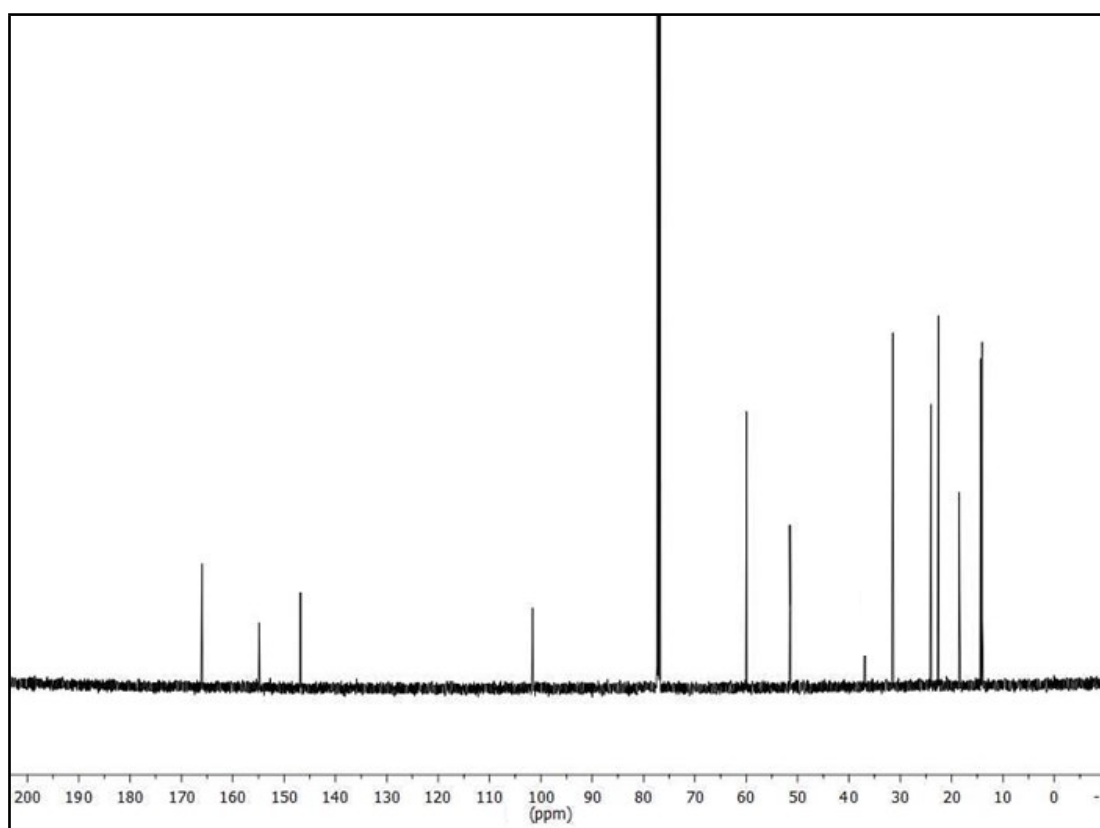
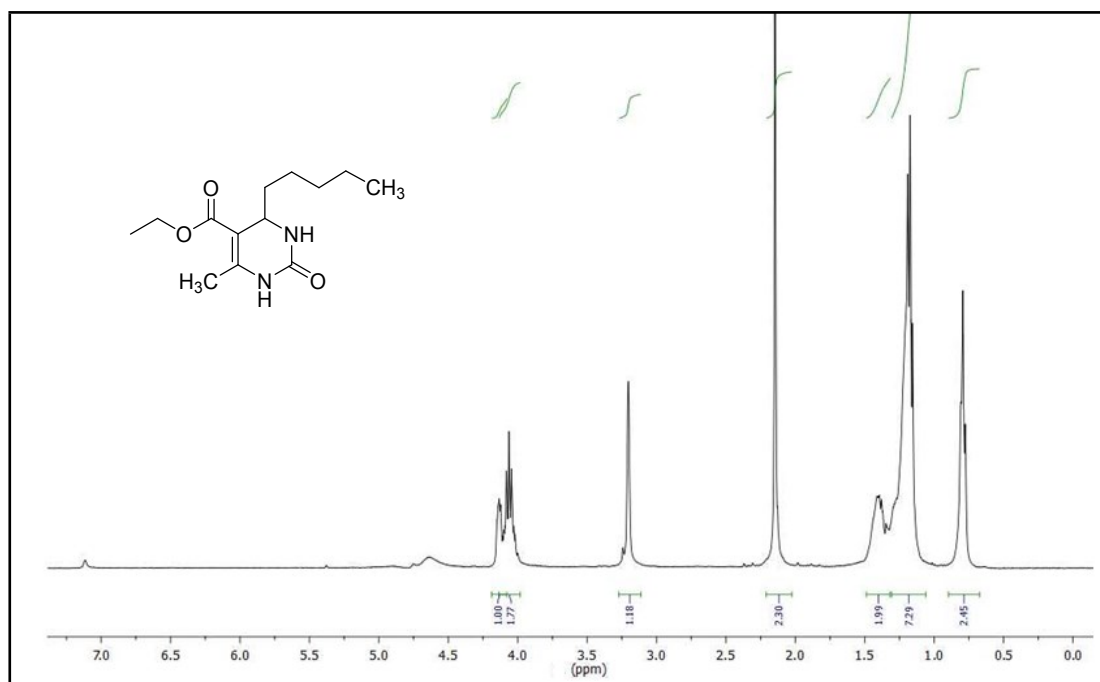
¹H & ¹³C NMR spectra of compound (5a)



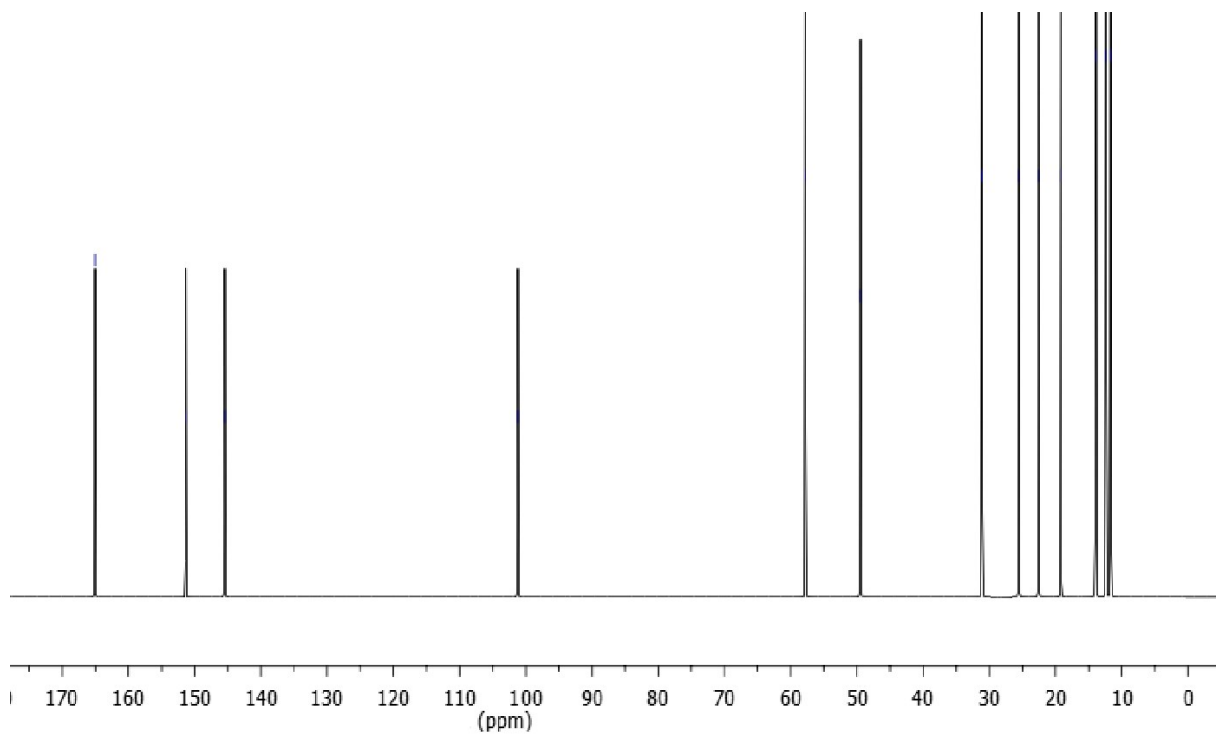
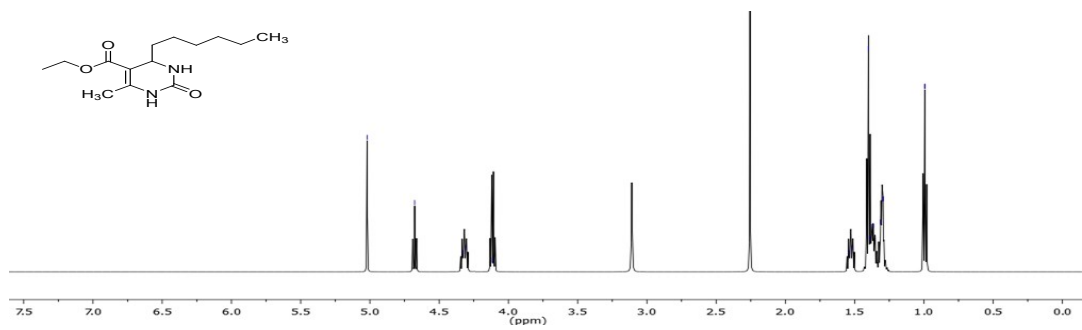
¹H & ¹³C NMR spectra of compound (6a)



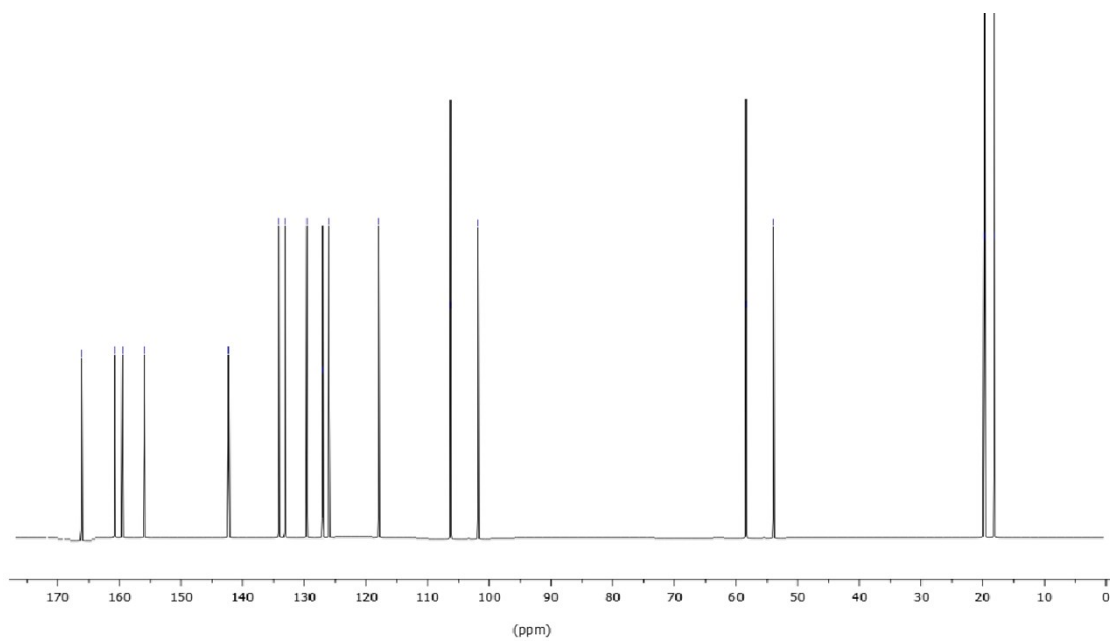
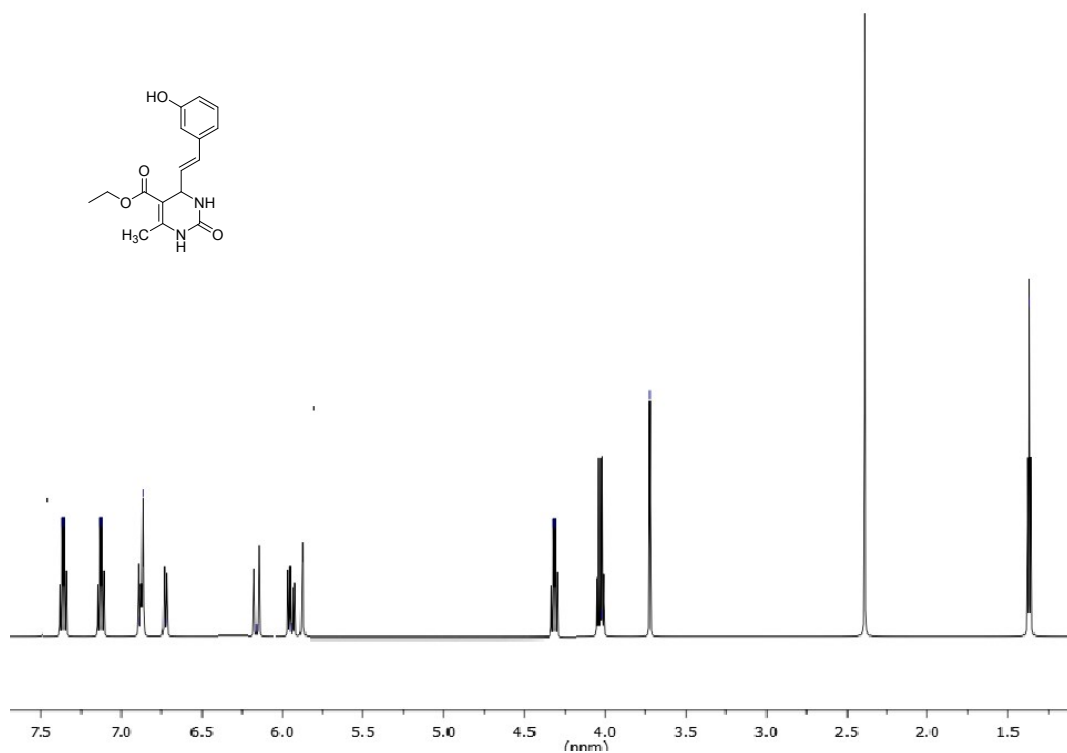
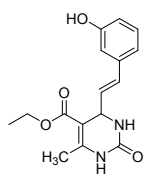
¹H & ¹³C NMR spectra of compound (7a)



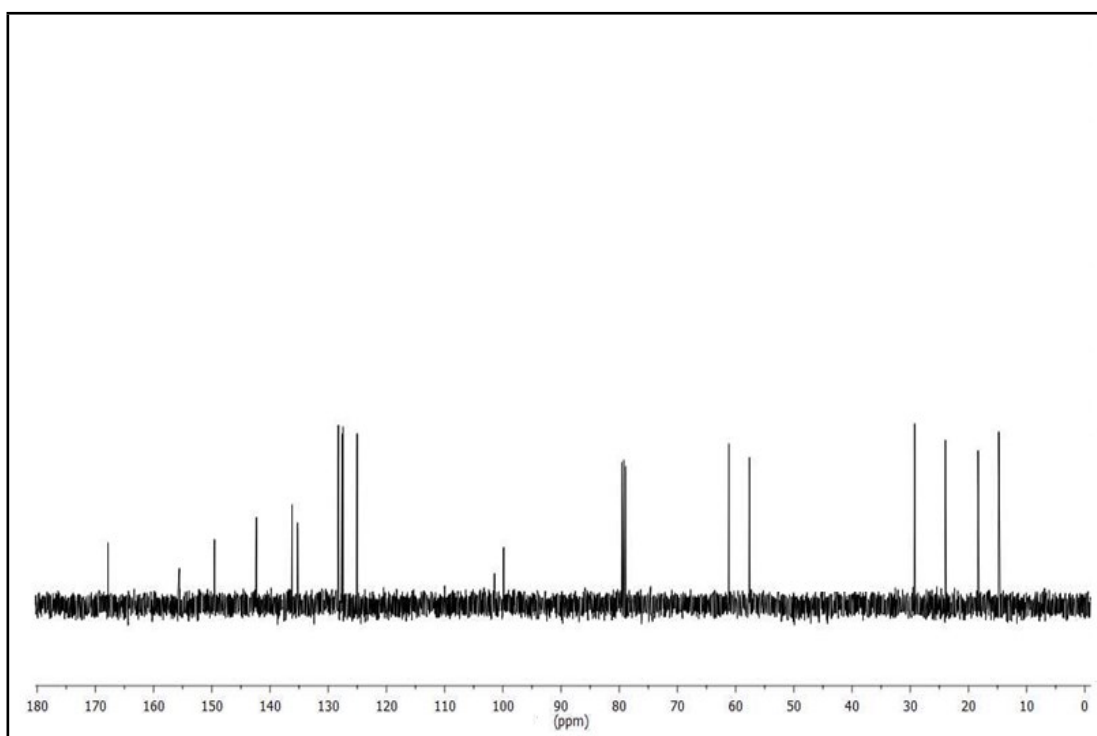
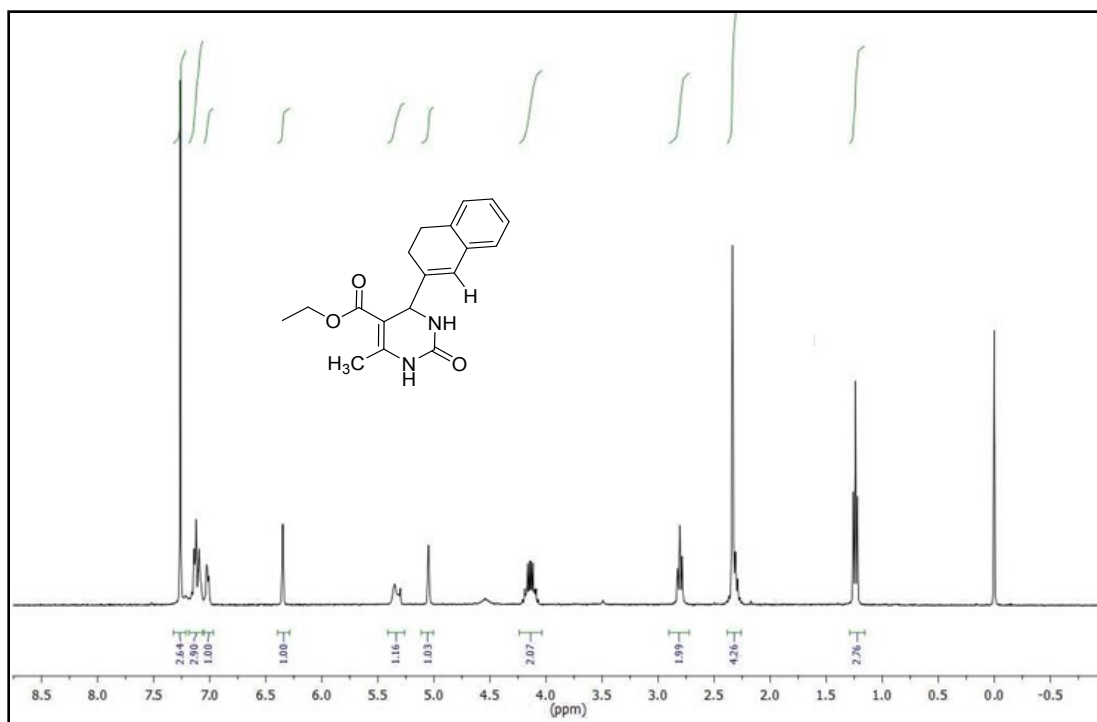
¹H & ¹³C NMR spectra of compound (8a)



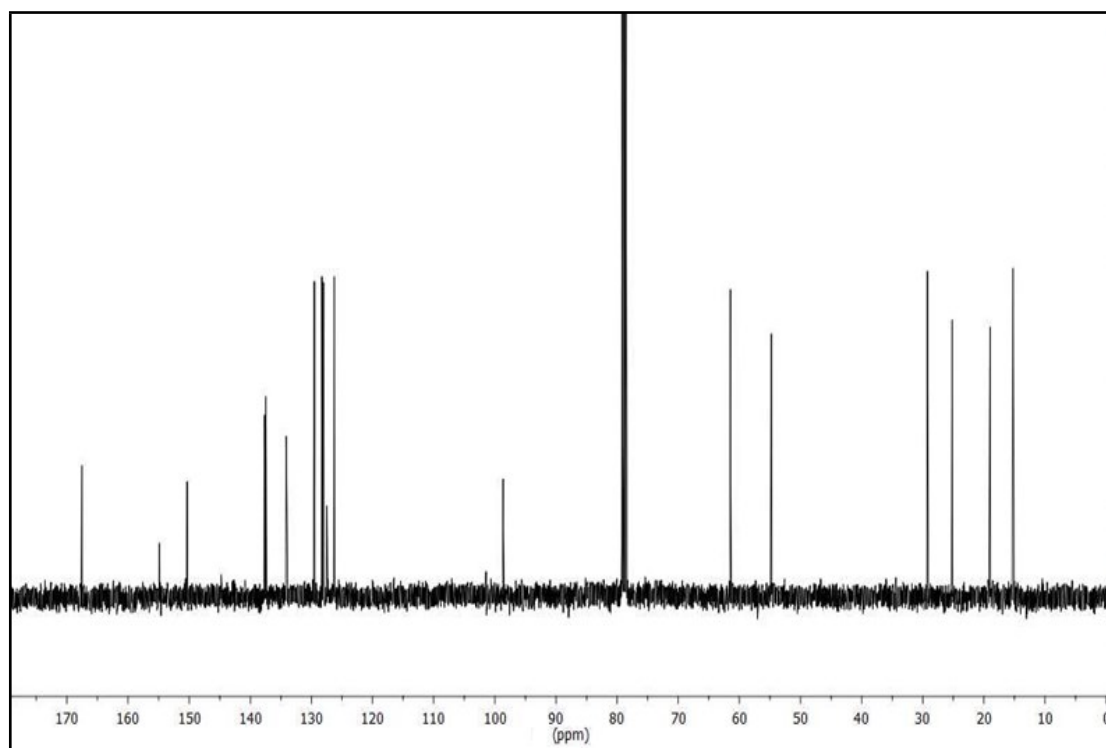
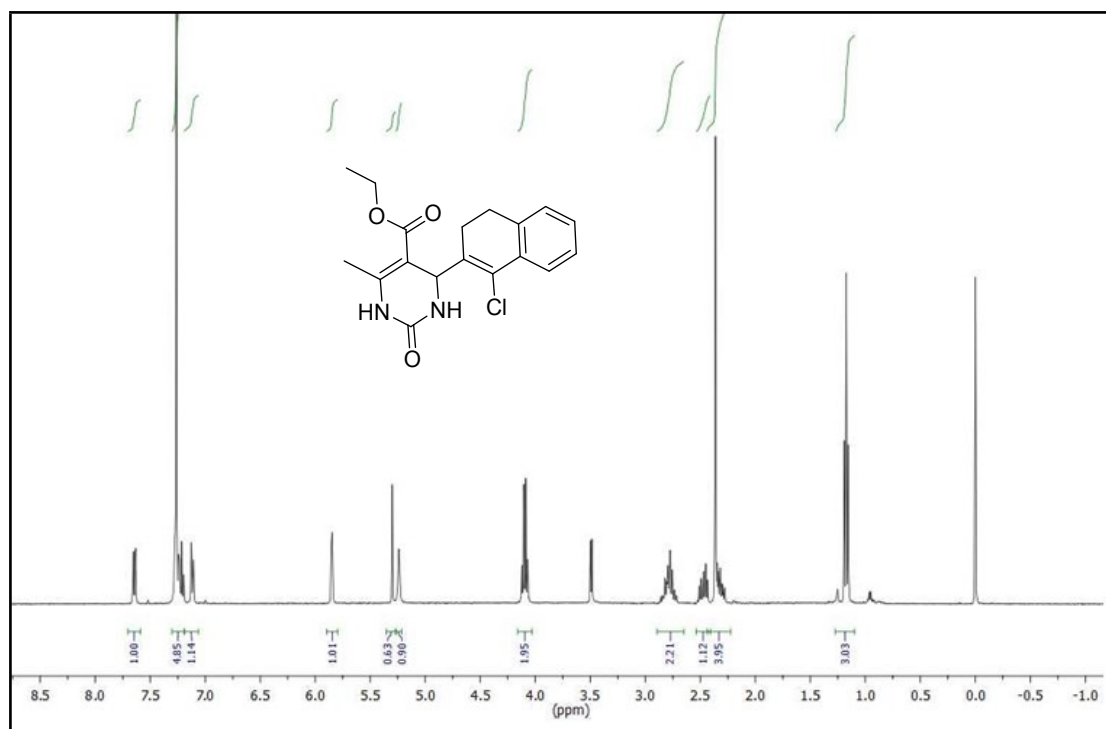
¹H & ¹³C NMR spectra of compound (9a)



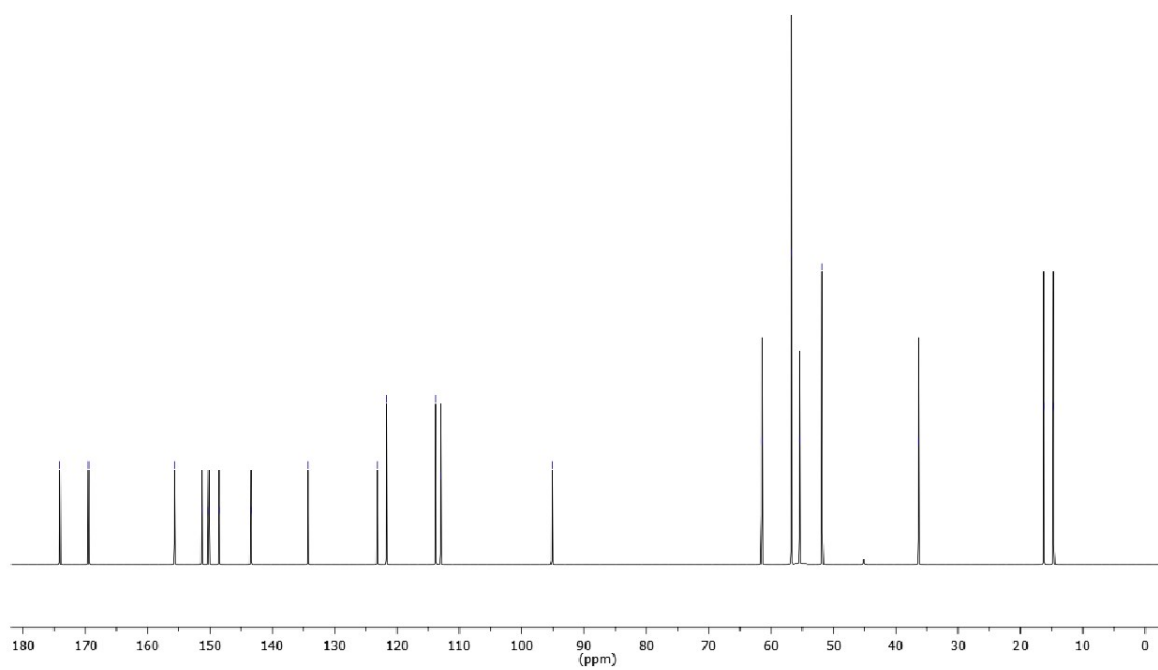
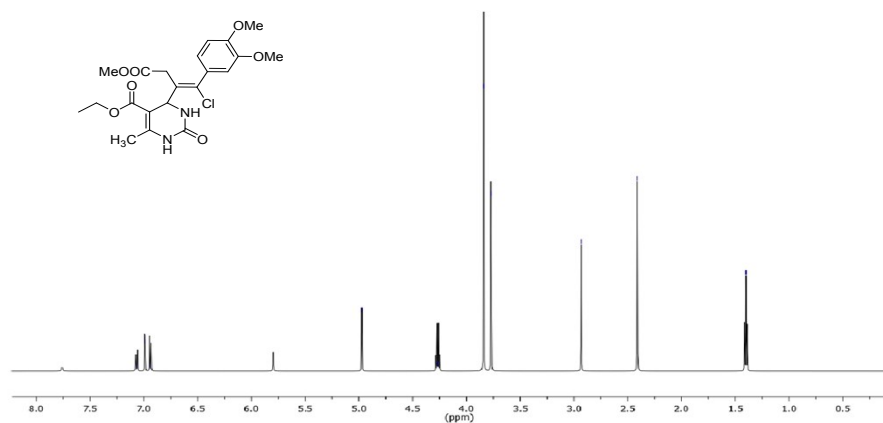
¹H & ¹³C NMR spectra of compound (10a)



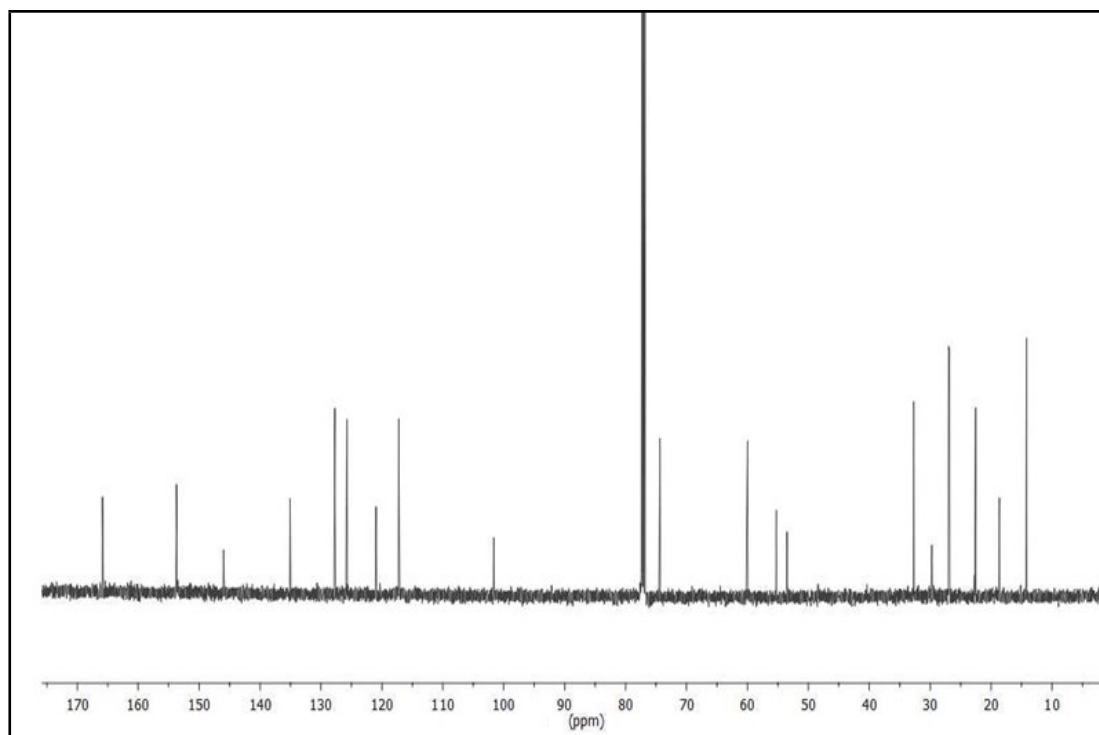
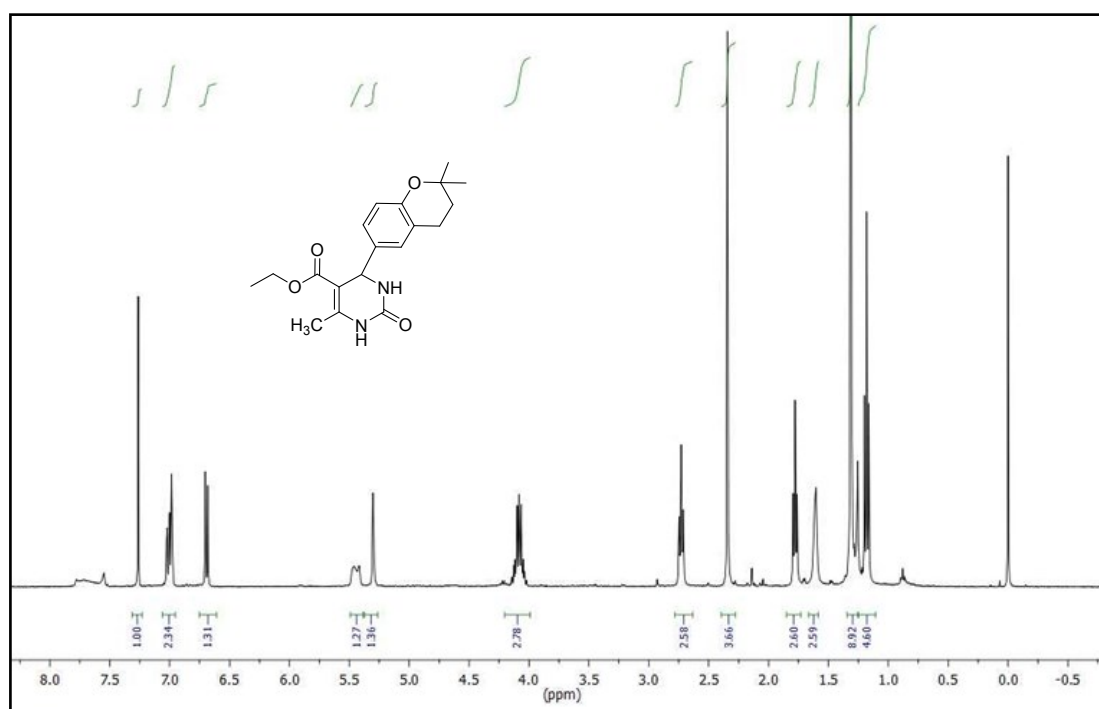
¹H & ¹³C NMR spectra of compound (11a)



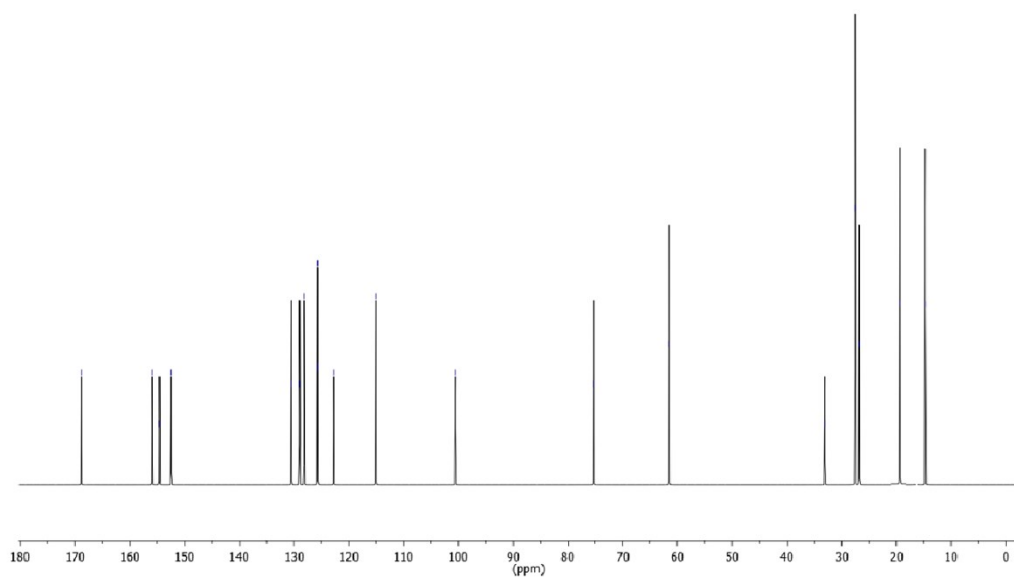
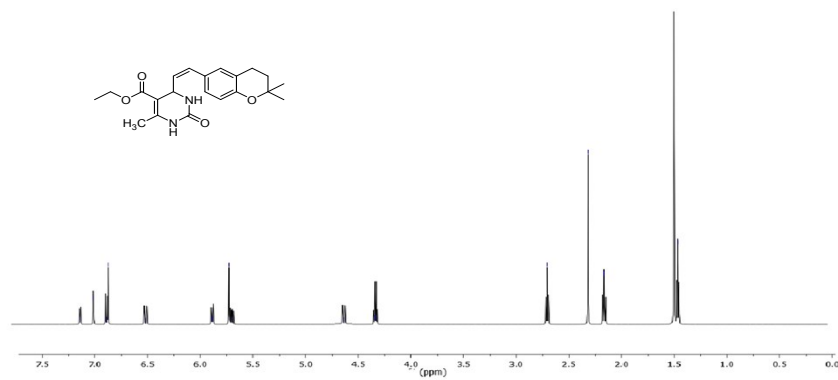
^1H & ^{13}C NMR spectra of compound (12a)



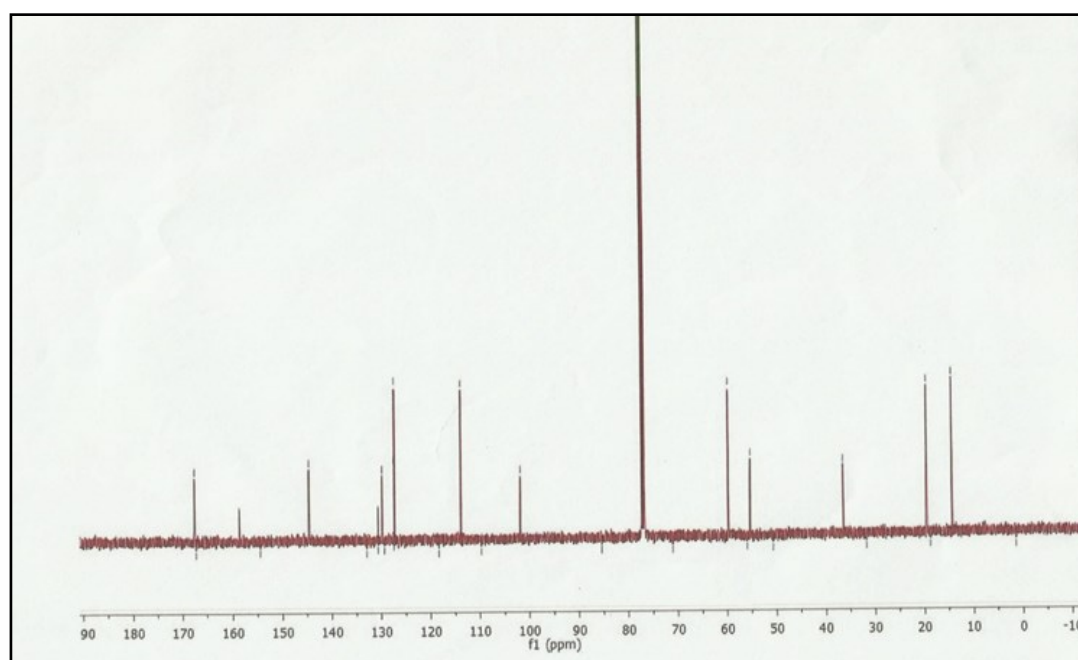
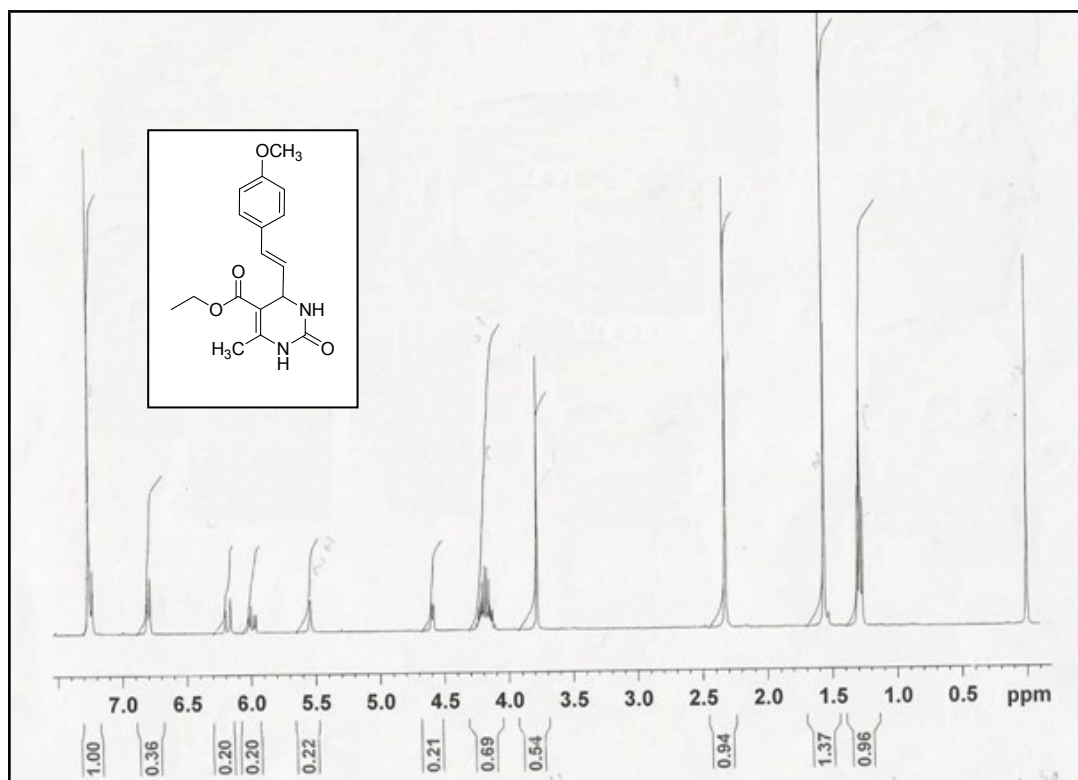
¹H & ¹³C NMR spectra of compound (13a)



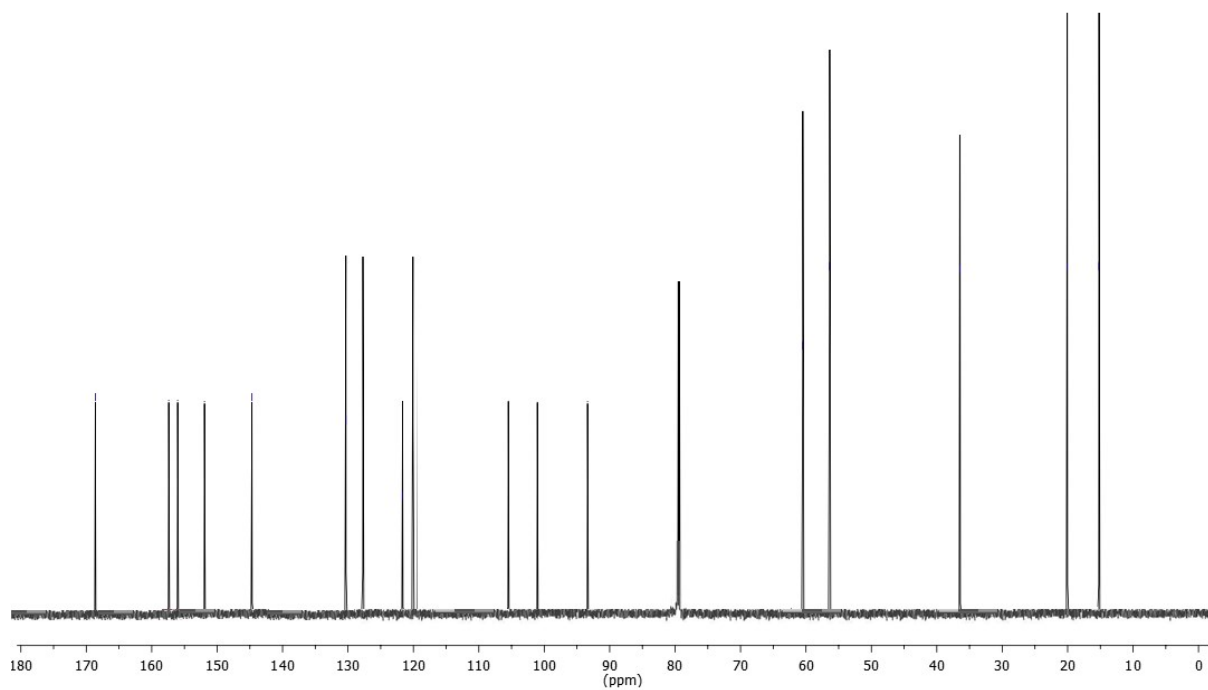
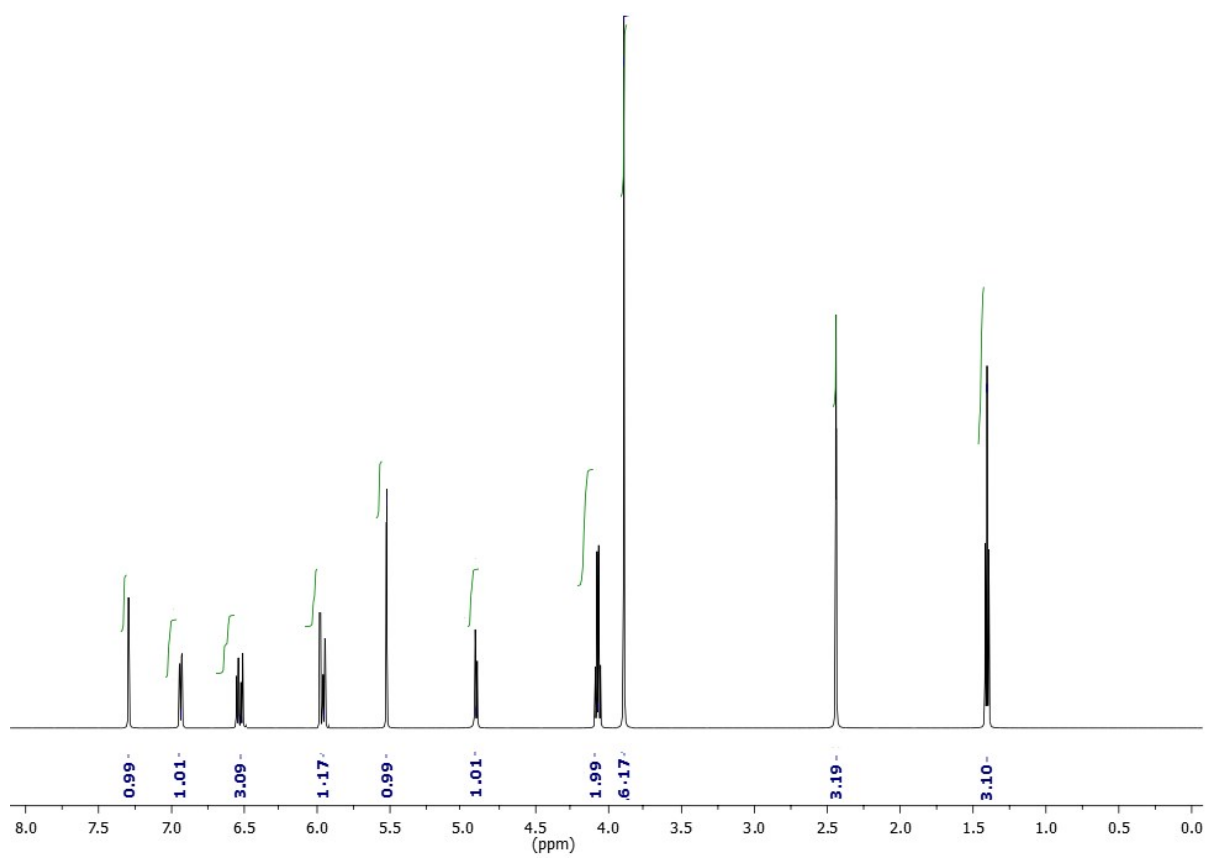
¹H & ¹³C NMR spectra of compound (14a)



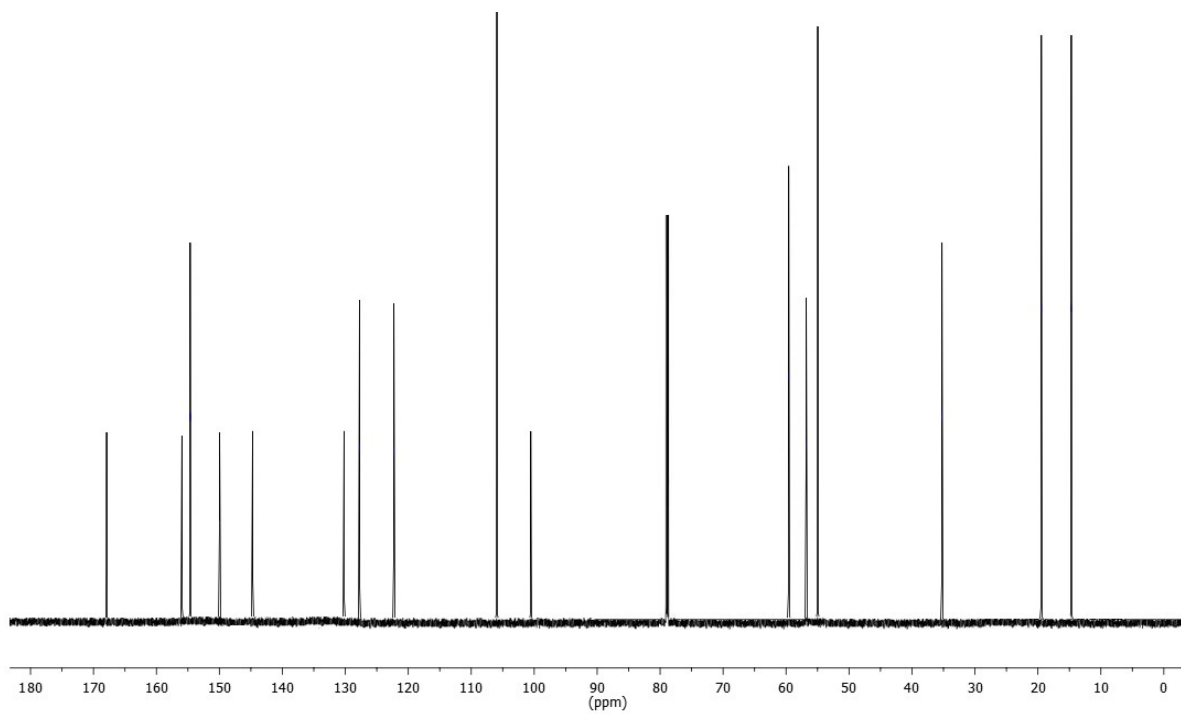
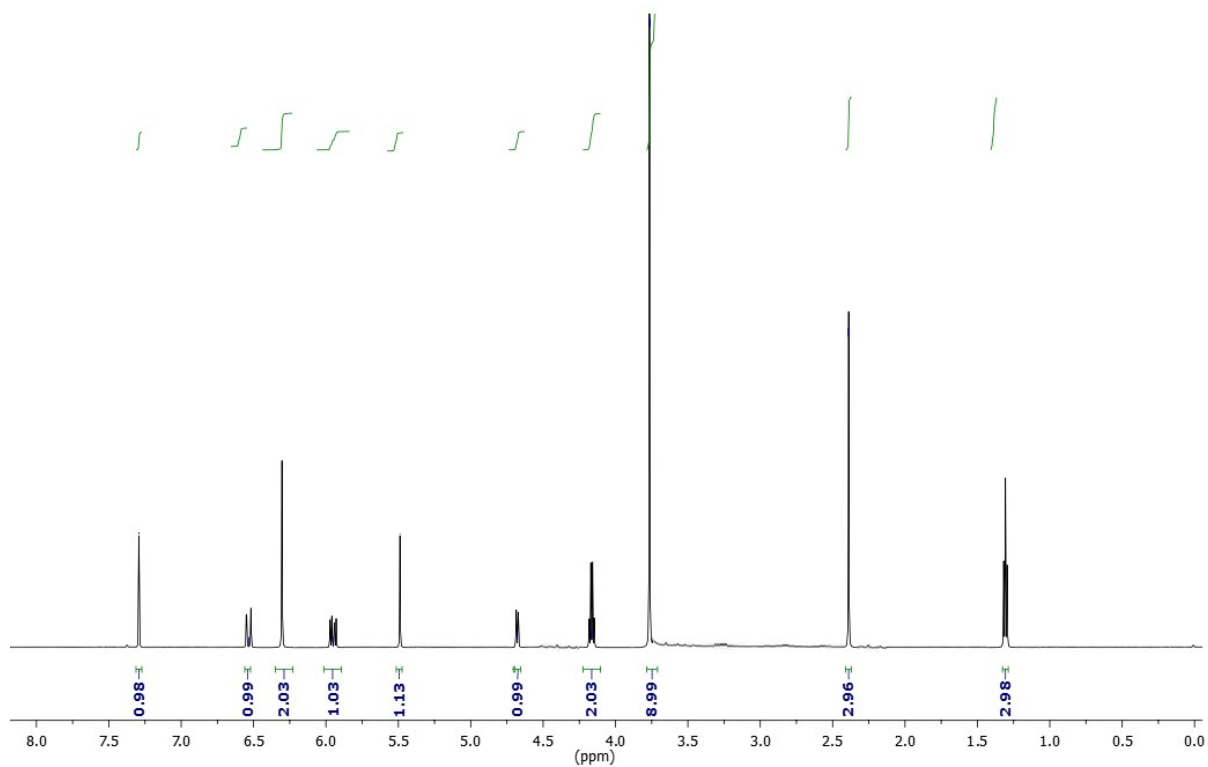
¹H & ¹³C NMR spectra of compound (15a)



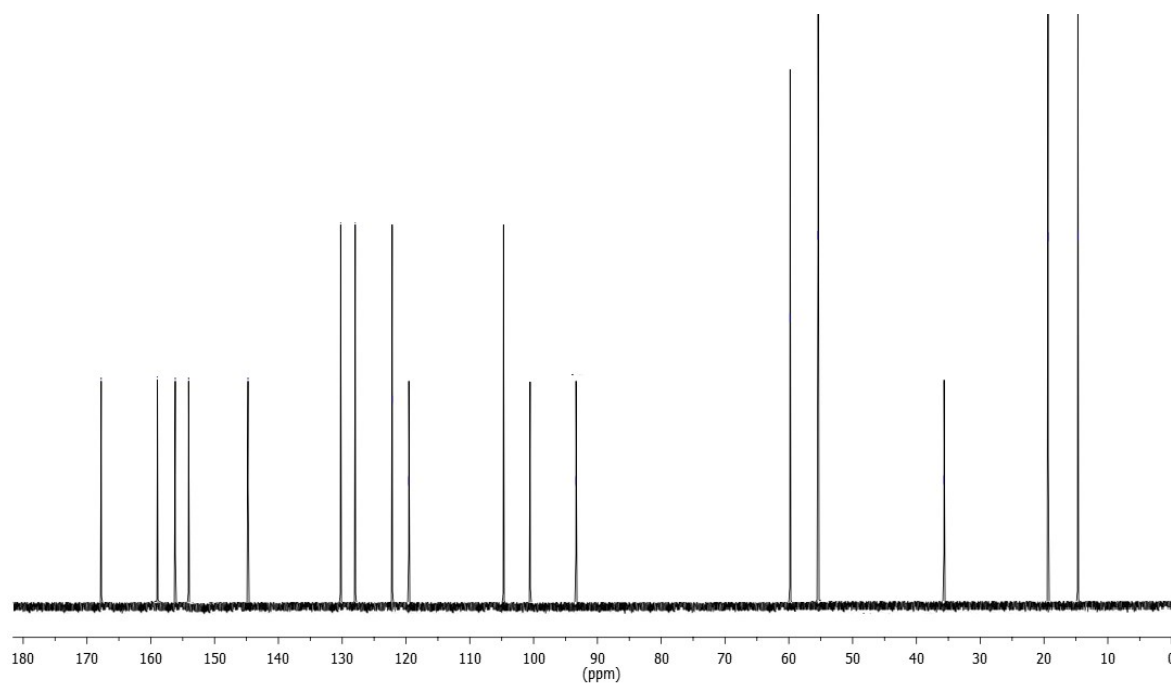
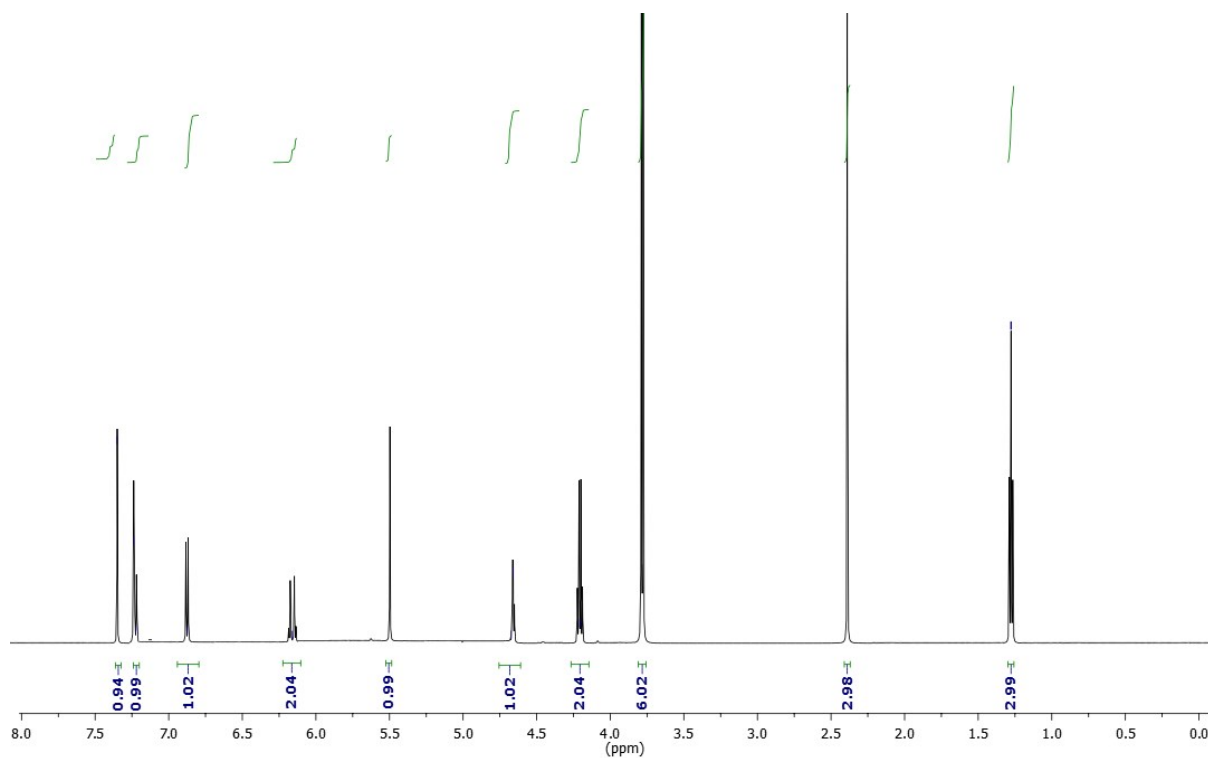
¹H & ¹³C NMR spectra of compound (16a)



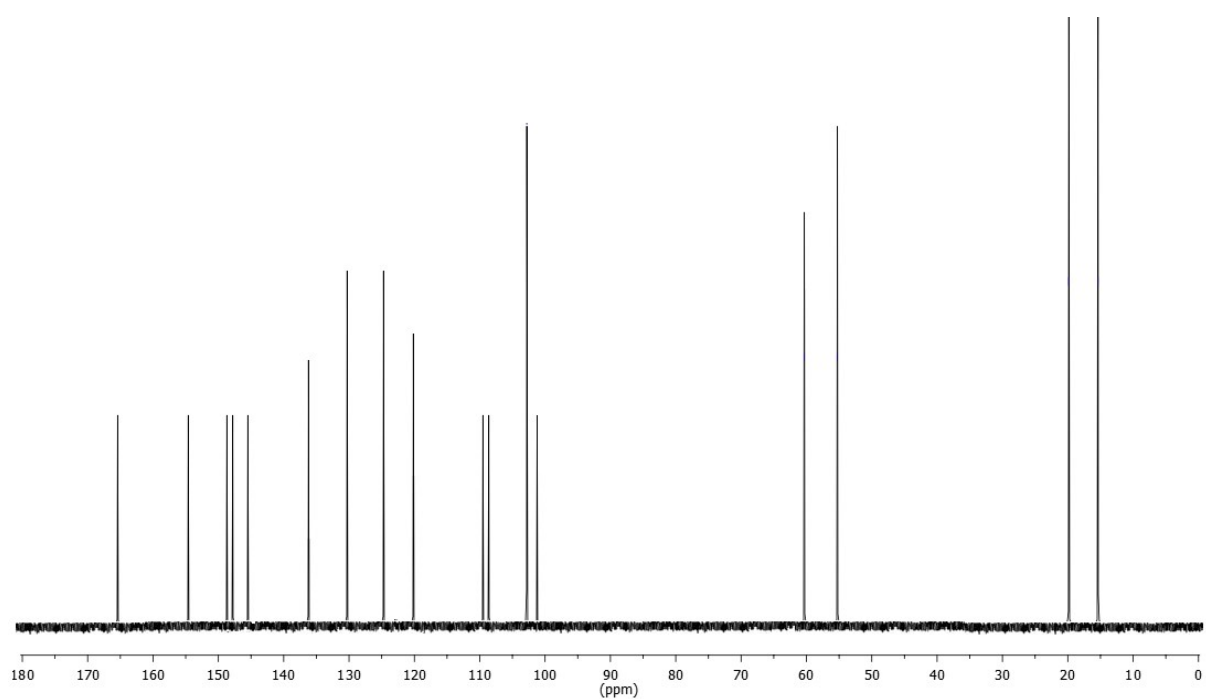
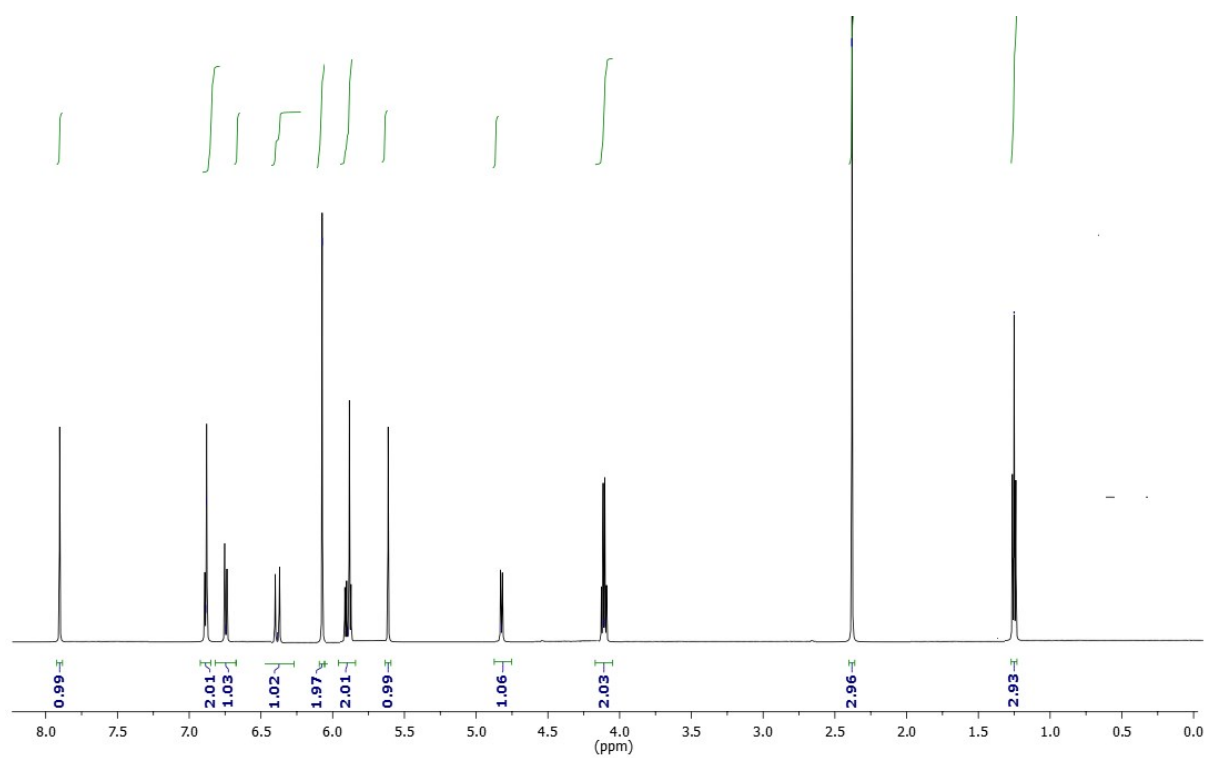
¹H & ¹³C NMR spectra of compound (17a)



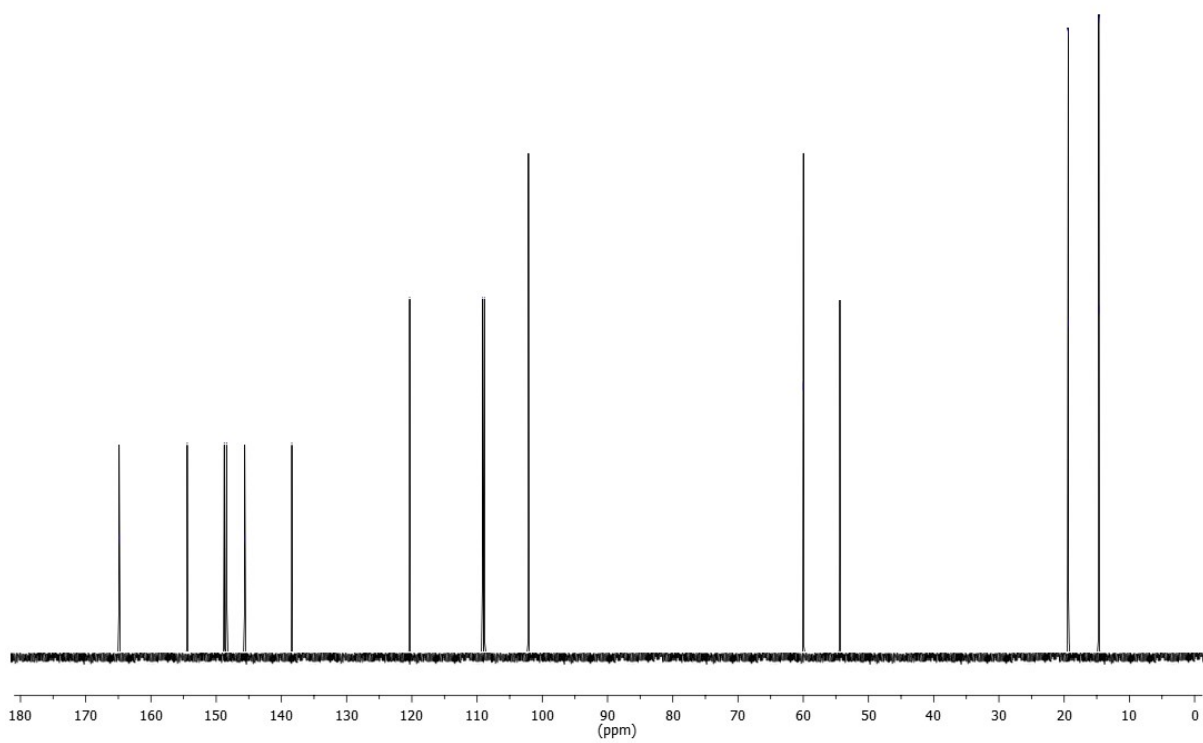
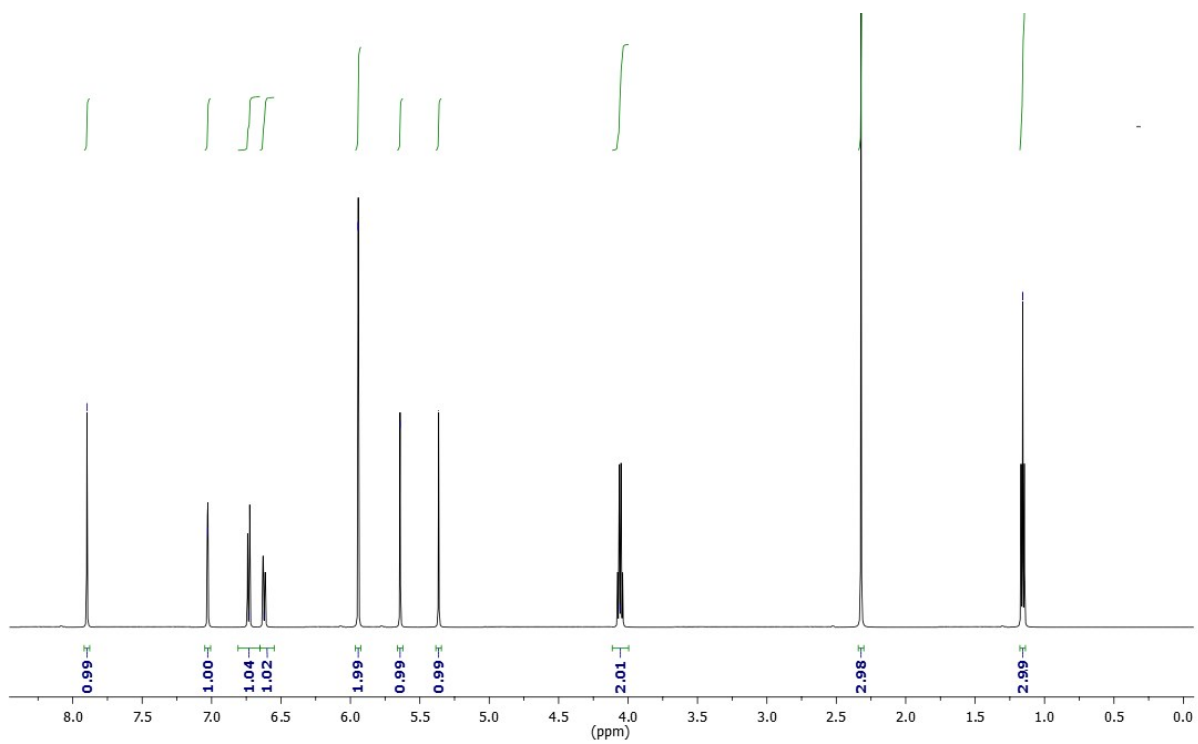
¹H & ¹³C NMR spectra of compound (18a)



¹H & ¹³C NMR spectra of compound (19a)



^1H & ^{13}C NMR spectra of compound (20a)



¹H & ¹³C NMR spectra of compound (21a)

Figure S6: Concentration dependent curves of synthesized Compounds

